General Disclaimer

One or more of the Following Statements may affect this Document

- This document has been reproduced from the best copy furnished by the organizational source. It is being released in the interest of making available as much information as possible.

- This document may contain data, which exceeds the sheet parameters. It was furnished in this condition by the organizational source and is the best copy available.

- This document may contain tone-on-tone or color graphs, charts and/or pictures, which have been reproduced in black and white.

- This document is paginated as submitted by the original source.

- Portions of this document are not fully legible due to the historical nature of some of the material. However, it is the best reproduction available from the original submission.

NASA CR–134882

GEORGIA INSTITUTE OF TECHNOLOGY
SCHOOL OF MECHANICAL ENGINEERING
Atlanta, Georgia

Investigations of Lubricant Rheology as Applied to Elastohydrodynamic Lubrication

NASA GRANT No.
11–002–133

By:
R. K. Kunz
H. S. Nagaraj
Graduate Students
D. M. Sanborn, Associate Professor
W. O. Winer, Professor
Co–Principal Investigators

For

NASA–LEWIS RESEARCH CENTER
21000 BROOKPARK ROAD
CLEVELAND, OHIO 44135

AUGUST, 1975

1. Report No.	2. Government Accession No.	3. Recipient's Catalog No.
NASA CR-134882		

4. Title and Subtitle	5. Report Date
INVESTIGATIONS OF LUBRICANT RHEOLOGY AS APPLIED TO ELASTOHYDRODYNAMIC LUBRICATION	August, 1975
	6. Performing Organization Code

7. Author(s)	8. Performing Organization Report No.
D. M. Sanborn, W. O. Winer, et al.	
	10. Work Unit No.

9. Performing Organization Name and Address	11. Contract or Grant No.
School of Mechanical Engineering Georgia Institute of Technology Atlanta, Georgia 30332	NGR11-002-133
	13. Type of Report and Period Covered
12. Sponsoring Agency Name and Address	Contractor Report
National Aeronautics and Space Administration Washington, D. C. 20546	14. Sponsoring Agency Code

15. Supplementary Notes

Project Manager, William R. Jones, Jr., Fluid System Components Division
NASA Lewis Research Center, Cleveland, Ohio

16. Abstract

This is the annual progress report for NASA Grant No. 11-002-133. The research under this grant consists of an analytical study of traction prediction in sliding EHD contacts and an elastohydrodynamic lubrication simulation study of the effects of load and speed on temperatures in the EHD contact. An existing shear stress theory and lubricant rheological model were studied and evaluated by applying them to traction prediction. Results obtained using measured film thickness and surface temperature data, were compared with measured traction values. The infrared technique for measuring temperatures in an EHD contact has been further developed and ball surface and fluid temperatures are reported for sliding speeds of 0.35 to 5.08 m/s at 0.52 to 2.03 GN/m^2 maximum pressure and surface roughnesses of .011 to .381 μm c.l.a. The relationship between asperity interaction, as measured by relocation surface profilimetry and high frequency temperature measurements, and the ratio of film thickness to surface roughness has also been studied.

17. Key Words (Suggested by Author(s))	18. Distribution Statement
Elastohydrodynamic Lubrication Pressure Viscosity Measurements Liquid Lubricants Lubricant Rheology	Unclassified - unlimited

19. Security Classif. (of this report)	20. Security Classif. (of this page)	21. No. of Pages	22. Price*
Unclassified	Unclassified	53	

NASA CR-134882

GEORGIA INSTITUTE OF TECHNOLOGY
School of Mechanical Engineering
Atlanta, Georgia

Investigations of Lubricant Rheology as Applied to Elastohydrodynamic Lubrication

NASA GRANT No.
11-002-133

by:

R. K. Kunz
H. S. Nagaraj
Graduate Students
D. M. Sanborn, Associate Professor
W. O. Winer, Professor
Co-Principal Investigators

For

NASA-LEWIS RESEARCH CENTER
21000 Brookpark Road
Cleveland, Ohio 44135

August, 1975

GEORGIA INSTITUTE OF TECHNOLOGY
School of Mechanical Engineering
Atlanta, Georgia

INVESTIGATIONS OF LUBRICANT RHEOLOGY AS APPLIED TO ELASTOHYDRODYNAMIC LUBRICATION

Ward O. Winer
Principal Investigator

David M. Sanborn
Principal Investigator

Stothe P. Kezios, Director
School of Mechanical Engineering

August, 1975

TABLE OF CONTENTS

NOMENCLATURE

a	Hertzian contact radius, m
C	Specific heat J/(kg K)
	a constant = 10^{-3} Ns/m^2
E	Characteristic fluid temperature, C
h	Film thickness, m
k	Thermal conductivity, W/(mK)
P	Pressure, N/m^2
Q	Temperature-viscosity coefficient
T	Temperature, C
TC	Traction coefficient
t_1	Thermal diffusion time, s
t_2	Characteristic fluid resident time, s
u_1, u_2, u_3	Velocities in the x_1, x_2, x_3 directions, m/s
V	Sliding velocity, m/s
W	Normal load, N
X_1, X_2, X_3	Cartesian coordinates, m
η	Viscosity, Ns/m^2
Λ	Ratio of film thickness to composite surface roughness, h/σ
ρ	Density, kg/m^3
σ	Composite surface roughness = $\sqrt{\sigma_b^2 + \sigma_s^2}$, μm
τ	Shear stress, N/m^2
ξ	Dummy integration variable

subscripts

1	Stationary surface
2	Moving surface
b	Ball surface
c	Contact center value
f	Fluid
H	Hertzian conditions
o	Ambient conditions or minimum value
s	Sapphire surface

I. SUMMARY

During the past year research in the areas listed below has progressed and is reported herein:

Prediction of Traction in Sliding EHD Contacts

The shear stress theory proposed in the previous report when applied to the sliding EHD point contact using a naphthenic oil was found to yield results consistent with experimental findings for the high end of the speed range studied. The particular speed at which this theory yields reasonable results depends on the normal load and film thickness. At lower speeds, the calculated tractions exceeded the measured values. This is possibly due to either the onset of asperity interaction as the film thickness decreased or the breakdown of the Newtonian fluid model at high shear stress.

Calculations based on the theory indicated that the traction tends to increase with an increase in base viscosity and a decrease in temperature viscosity dependence of the lubricant. A weaker traction increase resulted from an increase in the pressure-viscosity dependence of the fluid. Variation in the thermal conductivity was found to have very little effect on the traction.

Experimental Investigations in Sliding EHD Contacts

A complete mapping of the average fluid and ball surface temperature has been obtained for the relatively high Hertz pressure level of 1.51 GN/m^2. The previous report contained similar data for 1.05 GN/m^2 Hertz pressure. These data are compared to yield a qualitative dependence of fluid temperature levels on Hertz pressure. Further studies of the ball surface temperature only were made at pressure levels from 0.521 to 2.03 GN/m^2.

The results of these studies are then compared with the flash temperature theories of Blok, Jaeger and Archard. Deviations from the predictions are then discussed.

A detailed study of the effect of surface roughness on EHD contact behavior has also been undertaken. Balls of three roughness values ranging from .011 to .381 μm c.l.a. were studied using both a surface profilimeter and the EHD contact simulator. Ball surface profiles were determined prior to running in the EHD contact, and then through the use of a relocation technique, the surface profiles were again measured after an EHD experiment. It was found that changes in the profiles, as a result of asperity interaction, were closely related to the ratio of the film thickness to composite surface roughness and the surface temperature level.

Finally, a technique has been developed which allows the determination of temperature fluctuations arising from individual asperity interactions. All previous temperature data has been time-averaged by the infrared detector. The high frequency fluctuations are shown to exist only in cases where asperity interaction occurs. It has also been found that the range of these fluctuations increases with a decreasing ratio of film thickness to composite surface roughness.

II. THE PREDICTION OF TRACTION IN SLIDING EHD CONTACTS

A. Introduction

The determination of the traction force in elastohydrodynamic contacts is of primary importance in the understanding of many lubricated mechanisms. The traction is defined as the force generated in the contact which resists relative motion of the bearing surfaces. This is directly related to the power loss in mechanical components such as gears, cams, and rolling element bearings. Traction studies are also motivated by a need to predict the onset of skidding in rolling element bearings. However, due to the physical complexity of the problem, no simple model describing quantitatively the generation of traction in an EHD contact has yet been generally accepted. Complications caused by the large role of thermal effects and by difficulties in finding a rheological model which is adequate at high pressures and shear stress have hindered simplified theoretical analysis.

A number of models for predicting traction have been proposed. Crook (1), Kannel and Walowit (2), and Allen, Townsend and Zaretsky (3) all assumed isothermal bearing surfaces in their models. Based on temperature measurements by Turchina, Sanborn and Winer (4) this condition appears to be physically violated, particularly when a great deal of sliding is present. Cheng and Sternlicht (5) and Cheng (6) included thermal effects in a numerical analysis dealing primarily with line contacts in the prediction of film thickness, pressure, and temperature. While these investigations give a great deal of insight into the effects of thermal behavior in the analysis, the complexity of the numerical iteration technique

limits the practical application of this model for traction prediction over a wide range of physical situations. Trachman and Cheng (7) predicted traction in line contacts in a numerical solution which included both thermal effects, and non-Newtonian rheological models. Archard and Baglin (8) assumed isothermal conditions, a Newtonian fluid, and an exponential pressure-viscosity behavior. Because of these assumptions, their model is limited to low sliding speeds where thermal effects are less important. Archard and Baglin derived non-dimensional groups from physical considerations and established a foundation on which solutions with thermal effects and different rheological models may be built.

Jakobsen and Winer (9-11) have taken thermal effects into account, while limiting to a few graphical steps the work required to find the shear stress at a point in a sliding EHD contact. The method is thus suitable for predicting tractions over a wide range of conditions while eliminating the restrictions imposed by the assumption of isothermal walls. In addition, Jakobsen and Winer (9,10,12) have proposed a Newtonian model for lubricant behavior, employing a power-exponential temperature-viscosity function. This model resulted from the correlation of measurements on a capillary viscometer at shear stress levels only 3-5 times less than the average shear expected in an elastohydrodynamic contact.

This study attempts to evaluate the shear stress theory and lubricant rheological model of Jakobsen and Winer (9-12) by applying them to traction calculation in a sliding elastohydrodynamic point contact, and comparing the calculated values to experimental measurements. The correlation is limited to a single naphthenic oil N1 (15). The theory is also used to predict the effect on traction of variations in the lubricant material properties.

B. Application of the Theory

The assumptions which form the basis for this theory are summarized here in the context of their application to a sliding EHD contact. The flow geometry, with major assumptions, is shown in Figure 1. Surface 1 is stationary, and surface 2 moves with constant velocity in the x_1 direction. According to both theory and experiment, the change in film thickness over most of an EHD contact is very small compared with the size of the contact. The bearing surfaces are therefore assumed parallel in the vicinity of the point at which the shear stress is being calculated, although the film thickness is allowed to vary from point to point. While temperature variations are recognized to exist in the x_1 and x_2 directions, the gradients of temperature in these directions are smaller than in the x_3 direction by about four orders of magnitude. Therefore, temperature is assumed to be pointwise independent of x_1 and x_2.

Because surface 2 is moving, the major portion of heat generated in the contact is carried away by this surface which justifies the assumption that the stationary surface is adiabatic. Over the major portion of the contact, the component of shear stress due to the pressure gradient is much smaller than that due to sliding motion. Consequently, the pressure is assumed pointwise constant. Detailed discussion of these assumptions is found in Jakobsen (9). In addition, body forces are neglected, and density and thermal conductivity of the lubricant are assumed constant.

A Newtonian rheological model of the lubricant, employing a linear relationship between shear stress and shear rate, is used. The viscosity-temperature dependence is expressed by the power-exponential relation

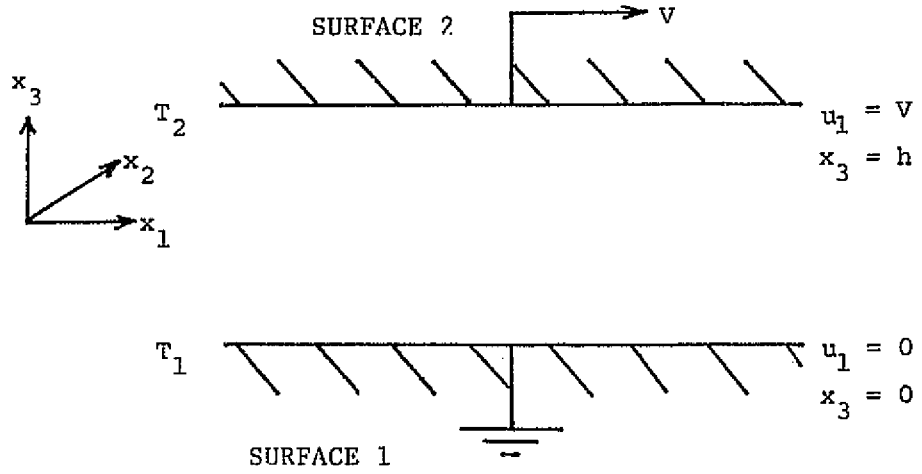

Assumptions

1. $u_1 = u_1(x_3)$; $u_1(0) = 0$, $u_1(h) = V$
2. $u_2 = u_3 = 0$
3. $T = T(x_3)$, $T(0) = T_1$; $T(h) = T_2$
4. constant pressure
5. constant density
6. constant thermal conductivity
7. steady state
8. laminar flow
9. body forces negligible

Figure 1. The Flow Geometry and Major Assumptions.

$$\eta = C \exp\left[(E/T)^{Q}\right] \tag{1}$$

both E and Q are functions of pressure. Jakobsen (9) has shown that this equation gives a reasonable description of lubricant viscosity within the range of temperature and shear stress normally found in an elastohydrodynamic contact.

Through integrations of the energy equation and the equations of motion, reduced by the above assumptions and the given rheological model, the theory provides a means of calculating the shear stress τ at any point in a sliding EHD contact. The condition of an adiabatic stationary wall yields the relation

$$\int_{T_1}^{T_2} \eta(T,Q)^{-1} dT = -\frac{V^2}{2k} \tag{2}$$

which is used to determine the temperature of the stationary surface, T_1. The shear stress at a point in the contact is then determined from the equation

$$\tau = -\frac{1}{2h} \int_{T_1}^{T_2} \left[-\frac{1}{2k} \int_{T_1}^{\hat{T}} \left[\eta(\xi,Q)^{-1} d\xi\right]^{-1/2} d\hat{T} \right] \tag{3}$$

The following parameters must be known: the temperature of the moving surface, T_2; the film thickness, h; the thermal conductivity of the fluid, k; the sliding speed, V; and the viscosity parameters Q and E. These latter two are calculated from the above equation and from viscometric data on the lubricant at the pressure of the point under consideration.

In order to perform this calculation, therefore, some assumption about the pressure distribution in the contact must be made. A Hertzian pressure distribution was chosen because of its simplicity for practical application, and its apparent applicability to a wide range of operating conditions. The computer-generated solutions to the EHD problem of Cheng and Sternlicht (5) show pressure distributions which converge to the Hertzian as the speed decreases and the load increases.

The procedure for calculating the shear stress at a point in the EHD contact is represented in the form of dimensionless charts in Jakobsen and Winer (11). The basic equations of the present theory were solved numerically. The traction in an EHD point contact was found by systematically calculating the shear stress throughout the Hertzian contact, and numerically integrating it over the contact area to yield the traction. Details of the numerical methods used, as well as a listing of the computer program, are given in Kunz (13).

C. Evaluation of the Theory

Measurements of traction for mineral oil N1 were made in a sliding EHD point contact using the equipment described in Sanborn and Winer (14), and the results compared to calculations using the methods described in the previous section. The contact consisted of a rotating steel ball whose surface was sliding with constant speed on a stationary flat surface of synthetic sapphire. The traction was measured for normal loads of 67 and 334 N, and sliding speeds ranging from .35 to 12.7 m/s.

The temperature distribution on the surface of the moving ball for each set of conditions was known from measurements made using the infrared technique described in Turchina, Sanborn and Winer (4). The

distribution of film thickness in the contact area was also known from measurements made using the optical interference method of Sanborn and Winer (15). The required pressure-viscosity data for the fluid N1 was obtained from Novak (16). Because viscosity data was only available at pressures up to 1.38×10^8 N/m^2, it was necessary to extrapolate the experimental curves up to the maximum Hertzian pressure of 1.0×10^9 N/m^2 for the 67N load, and 1.7×10^9 N/m^2 for the 334N load. This extrapolation was performed using Roelands' (17) pressure-viscosity correlation.

Figure 2 shows a plot of both calculated and measured tractions against sliding speed for the 67 N load. The traction is represented in the form of a traction coefficient, defined as the ratio between the traction force and the normal load. Figure 3 is a similar plot for the 334 N load. Figures 2 and 3 both indicate that the agreement between calculated and measured traction becomes better as the sliding speed increases. Because the film thickness decreases as the sliding speed decreases, there is a possibility that the divergence at lower speeds is related to asperity interaction. Such interaction could affect the contact in basically two ways which would tend to decrease the actual traction below the calculated values, as is observed in the figures. First, the contact between asperities could act as an additional source of heat which would raise the film temperature, and in turn lower the lubricant viscosity and therefore the traction. The traction model used in the calculations assumes that the only source of heat in the EHD contact is that due to viscous shearing of the lubricant. Therefore, one could expect calculated tractions to exceed the measured values. In addition, as the film thickness decreases and asperities come into contact, the asperities themselves would be

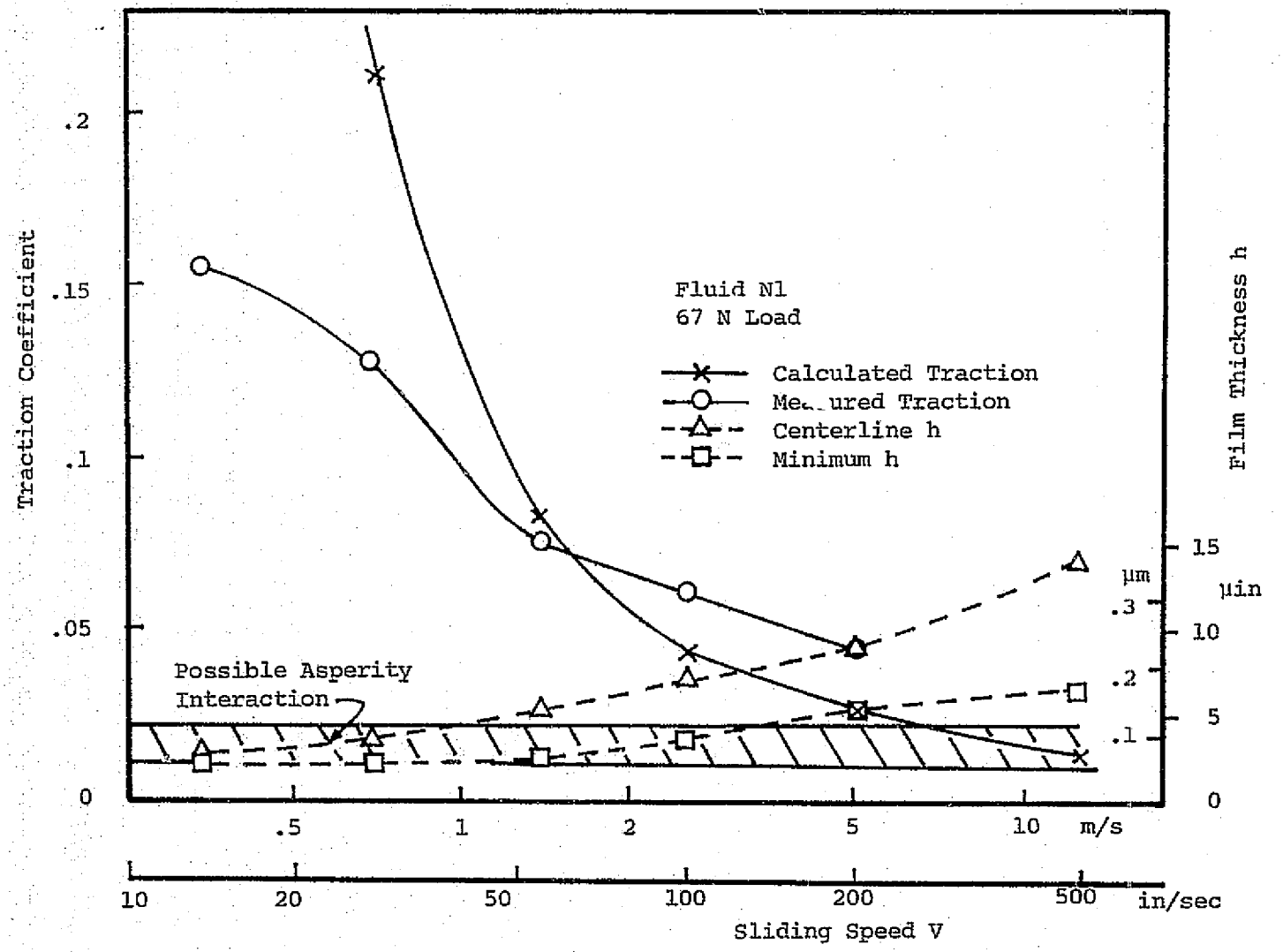

Figure 2. Calculated and Measured Traction - 1.0 GN/m^2 Hertz Pressure.

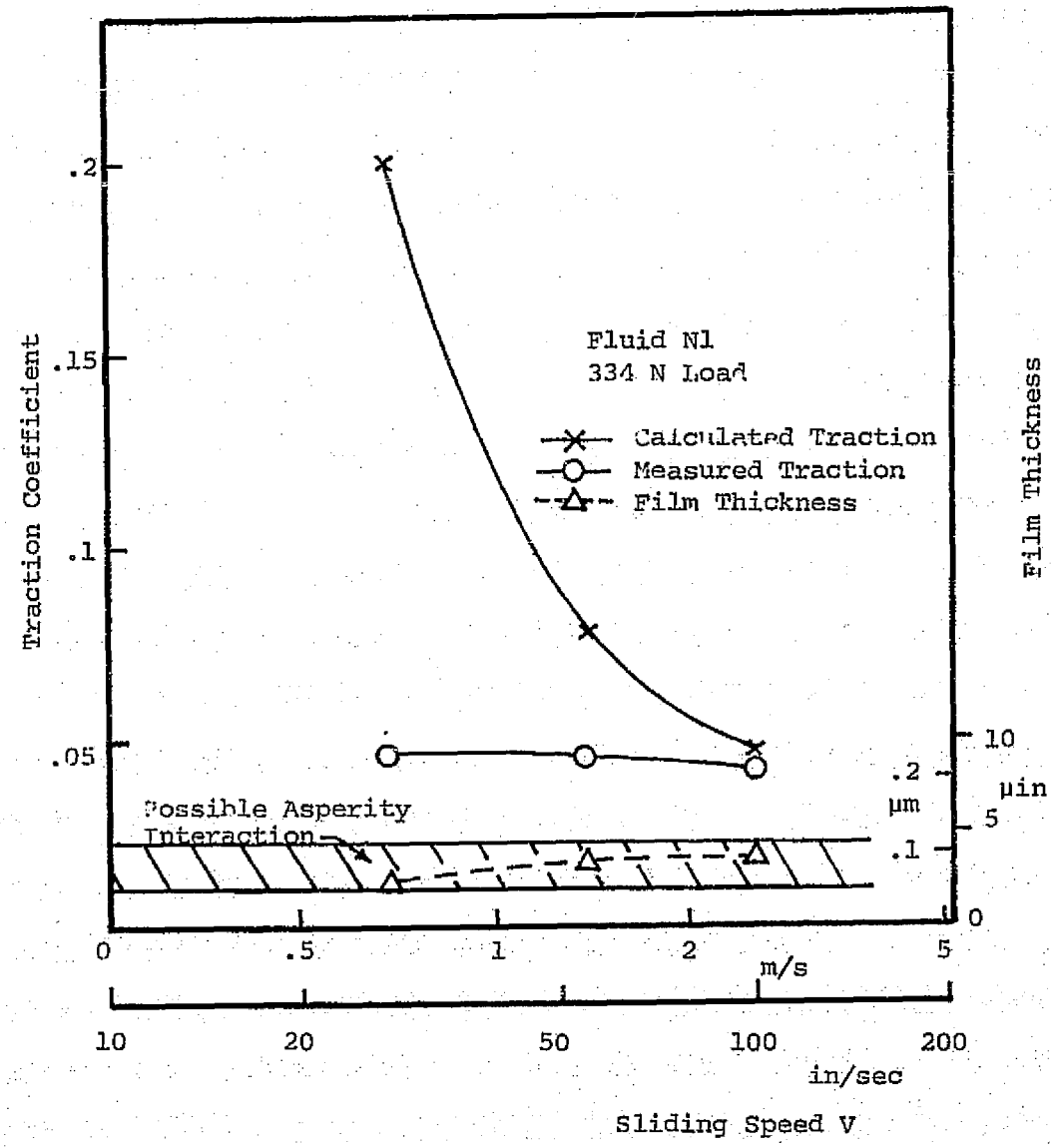

Figure 3. Calculated and Measured Traction - 1.7 GN/m^2 Hertz Pressure.

carrying a part of the load. This would result in lower pressure on the fluid, and therefore lower viscosity and a lower measured traction than predicted. Asperity interaction could cause traction to increase with some surfaces, but in the present case the surfaces were hard (52100 against sapphire) which minimized plowing and shearing effects.

In order to further investigate the possibility of asperity interaction, surface profiles of the steel ball and the sapphire were recorded on a profilometer. A composite rms surface roughness of about .046 μm was found for the two surfaces. A study by Sibley (18) indicates that some asperity interaction may be expected when the ratio Λ of film thickness to composite surface roughness is less than approximately 2.5. Recent surface temperature measurements in this laboratory (see Section III) indicate that asperity interaction begins to influence surface temperatures as Λ becomes one or less. Accordingly, the measured film thickness at each speed is shown in Figures 2 and 3, along with the region cross hatched which indicates a Λ of from 1 to 2.5. If the film thickness is below the cross hatched region, asperity interaction is certain to occur.

Another consideration in explaining the disparity between calculated and measured results is the behavior of the fluid under the extreme conditions imposed by a low sliding speed. It may be unreasonable to assume that a single rheological model is adequate to describe lubricant behavior throughout such a wide range of operating conditions. Johnson and Roberts (19) suggest that, above some critical shear stress, the fluid film behaves in the manner of a plastic solid rather than a viscous liquid. The possibility therefore exists that the rheological model used in this work breaks down when the shear stress in the film reaches some maximum

limiting value. The Johnson and Roberts limiting shear stress model would result in tractions closer to the measured values than the present model if the limiting shear stress of the fluid is less than the values calculated with the present model.

For the 67 N load, the maximum shear stress calculated at 1.40 m/s was in the neighborhood of 8.0×10^7 N/m^2. Similarly, for the 334 N load at 2.54 m/s, the maximum shear stress in the contact was calculated to be 8.1×10^7 N/m^2. Each of these two cases corresponds to the transition speed at which calculated and measured tractions began to deviate as the speed decreased. At higher speeds, calculated shear stresses were lower than these values throughout the contact. At speeds lower than the transition speeds, these shear stresses were exceeded by the calculated value. The fact that these maximum shear stresses are essentially the same for the two loads lends credence to the possibility that the Newtonian rheological model of the lubricant used in the calculations fails to adequately describe fluid behavior at extremely high shear stresses.

D. The Effect of Material Parameters on Traction

The effects on the traction of variations in the lubricant material parameters: temperature-viscosity dependence, pressure-viscosity dependence, base or inlet viscosity, and thermal conductivity were studied. These quantities were varied independently in calculations using the measured surface temperature and film thickness found for Fluid N1 (the naphthenic base oil (15)). The results were then compared with the calculations for Fluid N1.

In order to examine the effect of temperature-viscosity dependence on the calculated traction, a model fluid having the same pressure dependence

and inlet viscosity as Fluid N1, but having an exponential temperature-viscosity coefficient $\left|\frac{1}{\eta}\frac{d\eta}{dT}\right|$ one-half that of N1 at inlet conditions was used in the program. The viscosity-temperature behavior of this model fluid is similar to that of a dimethyl siloxane, a lubricant with low temperature-viscosity dependence, but the pressure-viscosity characteristics are quite different. The resulting calculated traction coefficient for a 67 N load and a speed of 2.54 m/s was three times greater than that calculated for Fluid N1 for the same load and speed conditions. The traction is therefore increased by a decrease in the temperature-viscosity coefficient of the lubricant, and appears to be fairly sensitive to such changes.

The pressure viscosity dependence was investigated by using a different means of extrapolating Novak's (16) viscosity data for Fluid N1 to the high pressures near the center of the contact. The shape of the pressure-viscosity curve was taken to be the same as that for a similar naphthenic fluid, (Fluid 36-G of the ASME Pressure-Viscosity Report (20) for which data was available up to 6.9×10^8 N/m^2. The viscosity thus obtained for the pressure at the center of the contact was three times less than that previously used for Fluid N1. The viscosity and temperature dependence at inlet conditions were taken to be the same as those for Fluid N1. The traction calculations using these viscosities were about 15% lower than those of Fluid N1 for the same load and speed conditions. This indicates that an increase in the traction would result from increases in the pressure-viscosity dependence, but that the traction is relatively insensitive to such changes.

The effect of the inlet viscosity on the traction was also studied.

Another model fluid was used, having the same pressure and temperature dependence as Fluid N1, but having a viscosity at inlet conditions three times that of Fluid N1. As before, all other system parameters were held constant. The resulting traction coefficient was greater than that for Fluid N1 by a factor of 1.75. The traction therefore increases as the inlet viscosity increases.

The only other lubricant material parameter involved in the traction calculation is the thermal conductivity. Variations in this property appear to have very little effect on the traction. In addition, the thermal conductivities for most hydrocarbon and dimethyl siloxane lubricants fall within a very narrow range.

Traction measurements would not be expected to be as sensitive to material property differences as the above calculations indicate. This is primarily because the surface temperatures for Fluid N1 were used in the calculations. Using a more viscous fluid, for instance, would increase the energy dissipation in the contact, thus increasing the temperature and decreasing the traction until a lower steady state value is reached with higher surface temperatures. Temperatures and film thicknesses for Fluid N1 were used only so as to allow independent variation of the material parameters. Consequently, the results of the calculations of this section should be viewed as relative variations only, rather than as absolute magnitudes to be expected in actual lubrication situations.

E. Conclusions

The shear stress theory of Jakobsen and Winer (11), when applied to a sliding EHD point contact, was found to yield realistic values for the traction at high sliding speeds. The particular speed at which the

theory becomes applicable depends on such factors as normal load and film thickness. At lower sliding speeds, the calculated tractions exceeded the measured values. This was possibly due either to the onset of asperity interaction as the film thickness decreased, or to the breakdown of the Newtonian fluid model at high shear stress.

Calculations based on the theory indicated that the traction tends to increase with an increase in base viscosity and a decrease in temperature viscosity dependence of the lubricant. A weaker traction increase resulted from an increase in the pressure-viscosity dependence of the fluid. Variation in the thermal conductivity was found to have very little effect on the traction.

III. EXPERIMENTAL INVESTIGATIONS IN SLIDING EHD CONTACTS

A. Temperature Distributions at a 215N Normal Load

The distribution of the average fluid film temperature and ball surface temperature, for a load of 67 N (1.05 GN/m^2 maximum Hertz pressure) have been obtained using the test apparatus shown in Figure 4 and the results were reported previously [10,21]. Similar measurements for the case of a normal load of 215N (1.51 GN/m^2 maximum Hertz pressure) were made and the most important results are given in Table I. It can be seen from Table I that the film thickness at the center of the EHD conjunction, at the side lobes and at the contact exit are all essentially the same. This constant film thickness tends to give more symmetric temperature distributions than previously observed.

In addition, at the higher load (215N), the maximum ball surface and fluid temperatures always occurred on or near the contact centerline at a point downstream of the contact center. The reason for this is that the pressure, and thus viscosity, is greatest at the contact center, and consequently, for a uniform film thickness, viscous dissipation is a maximum at the center. However, since the fluid residence period increases as it moves toward the exit, the position of the maximum temperature could be between the contact center and exit depending on the effectiveness of heat transfer at the bearing surfaces. At lower loads [10], the maximum contact temperature may occur off the contact center line, for example, at the side lobe constriction. This is attributable to the very low film thicknesses at the side lobes compared to other locations.

Also, the position of the maximum fluid film temperature is upstream of the position of the maximum ball surface temperature. Keeping in mind

Table I. Summary of Experimental Results for 215N Normal Load
(1.51 GN/m^2 = 219 kpsi peak Pressure)
For 0.012 μm (0.45 μ-in.) Cla. ball.

Speed m/s	h_c μm	h_o Sidelobe min μm	h_o CenterLine min μm	Temp. at Inlet-°C		Temp. at Center-°C		Temp. Centerline Max °C		Temp. Sidelobe max °C	
				Ball	Fluid	Ball	Fluid	Ball	Fluid	Ball	Fluid
0.70	0.065	0.065	0.065	67	155	136	212	149	217	76	168
1.39	0.088	0.088	0.088	85	163	156	224	175	226	110	186
2.54	0.088	0.088	0.088	91	177	187	243	197	246	No Sidelobe max.	

(Fluid N1, Load 215N (peak Pressure = 1.51 GN/m^2), Bath Temp. 40± 1C).

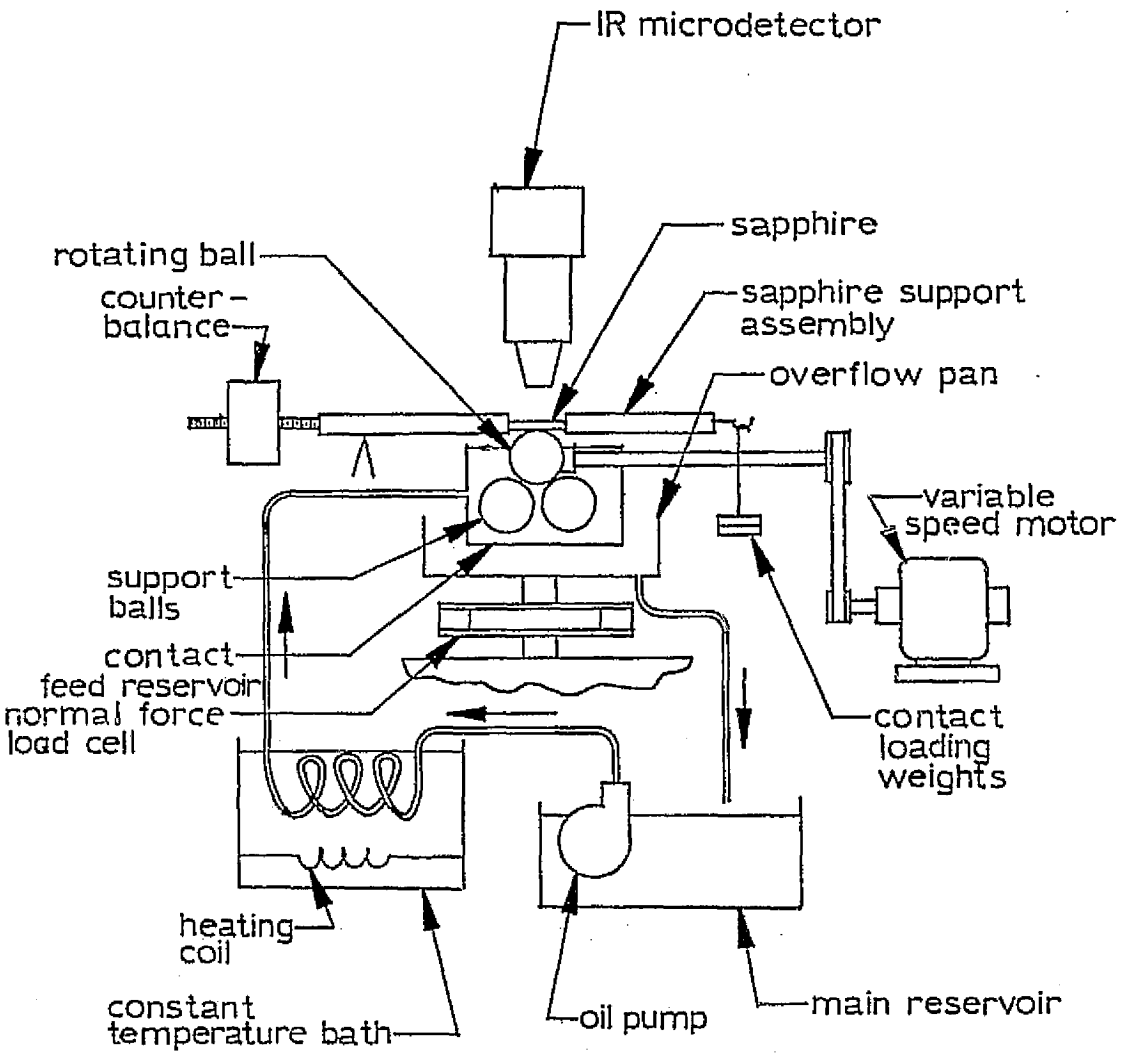

Figure 4. Sliding EHD Test Apparatus.

that the fluid film temperatures are essentially fourth power averages through the film, the observed shift in peak temperatures does not imply a violation of physical principles since the fluid temperature gradients at the ball surface may change considerably with position along the centerline allowing a matching of ball and fluid temperature levels at the interface.

Figures 5 and 6 show temperature contours for a sliding speed of 1.39 m/s. The general shape of the ball surface temperature contours (Figure 5) is similar to that found at lower loads [10]. In the present case, the ball surface enters the Hertzian contact at 85 C and reaches a maximum of 180 C downstream of the contact center. The fluid temperature contours shown in Figure 6 show that the difference between the primary maximum (226 C) on the centerline and the secondary maximum (186 C) in the side lobes has significantly increased compared to the lighter load of 67N [10]. In the lighter load case, the temperatures were 171 C and 173 C respectively. At 215N, the secondary maximum disappears as the speed is increased.

Figures 7 and 8 show respectively the ball surface and fluid temperatures along the centerline for a range of speeds. Results for the 67N load are also shown. The difference between the nature of the temperature distribution along the centerline for the two loads is attributable to different shapes of the film thickness profiles. The nearly constant film thickness at the 215N load yields fluid temperatures, which like the ball temperatures in both cases, change smoothly along the centerline.

Figure 9 shows the inlet temperature increase as functions of speed for the fluid and ball surface at the higher load condition. Temperatures

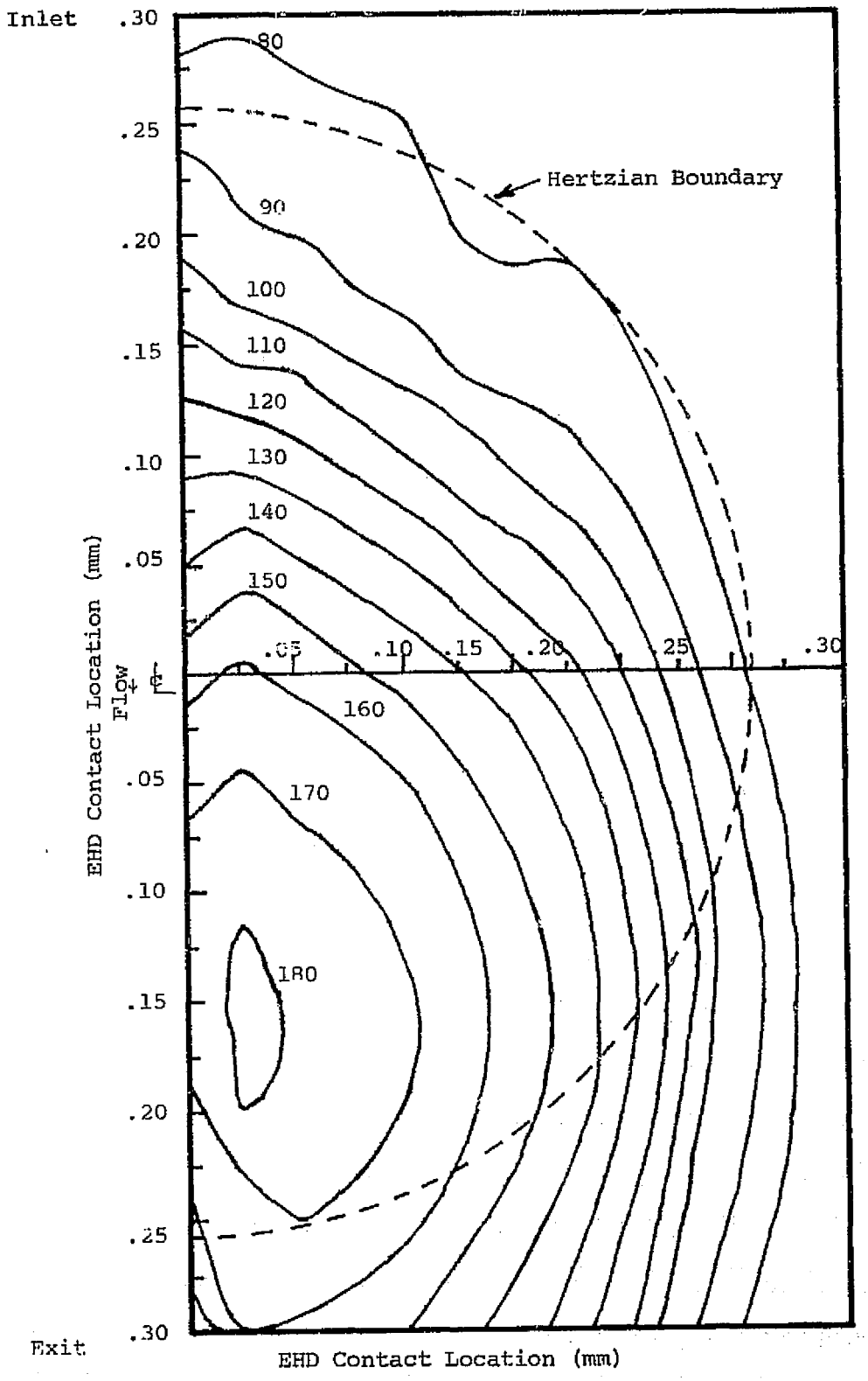

Figure 5. Ball Surface Temperature ($^{\circ}$C) - 1.05 GN,m^{2} Hertz Pressure, Naphthenic Base Oil, 40°C Bath Temperature, 1.39 m/s Sliding Speed, Smooth Ball (0.011 µm c.l.a.)

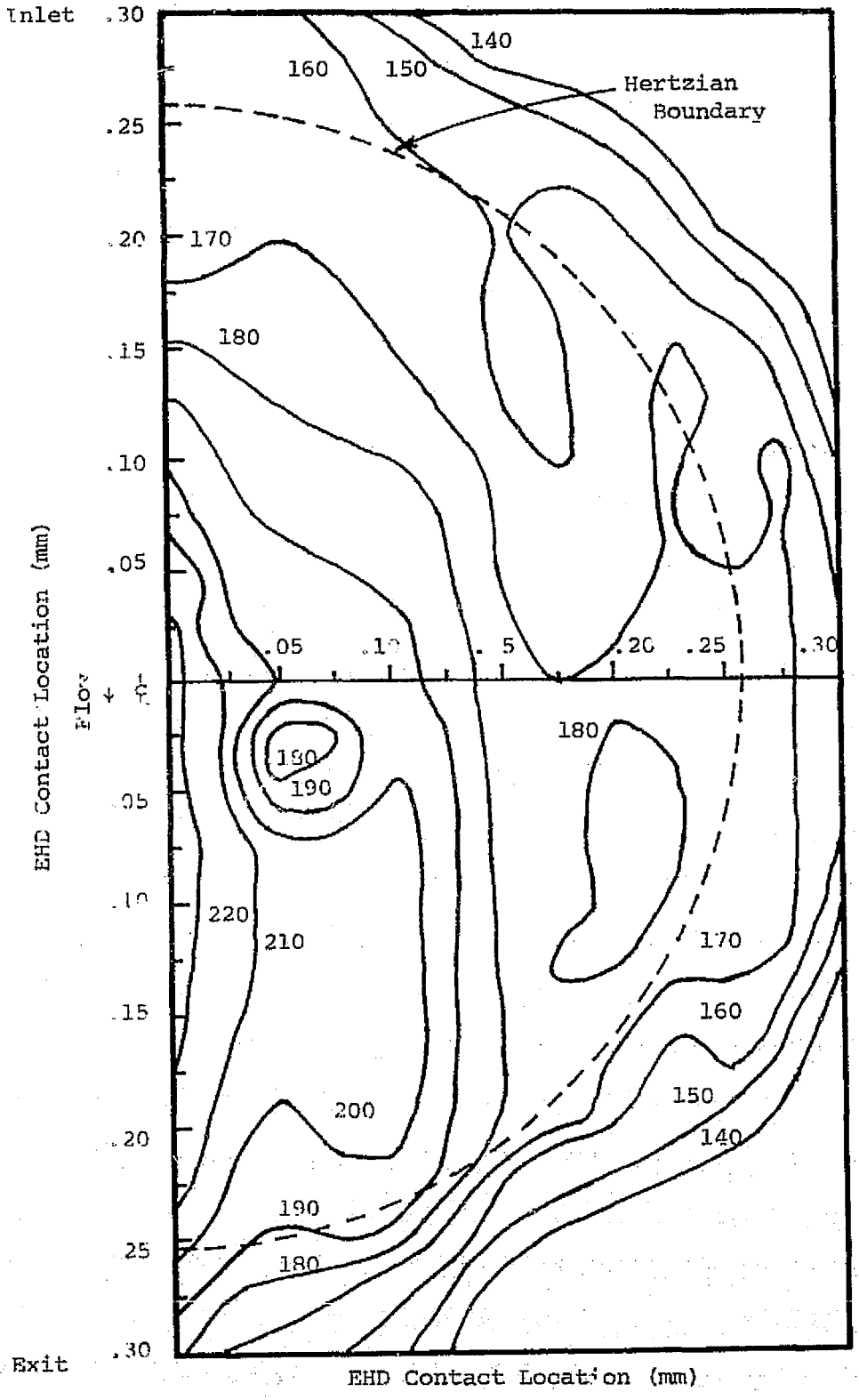

Figure 6. Average Fluid Temperature (^{o}C) 1.05 GN/m^{2} Hertz Pressure, Naphthenic Base Oil, 40^{o}C Bath Temperature, 1.39 m/s Sliding Speed, Smooth Ball (0.011 μm c.l.a.).

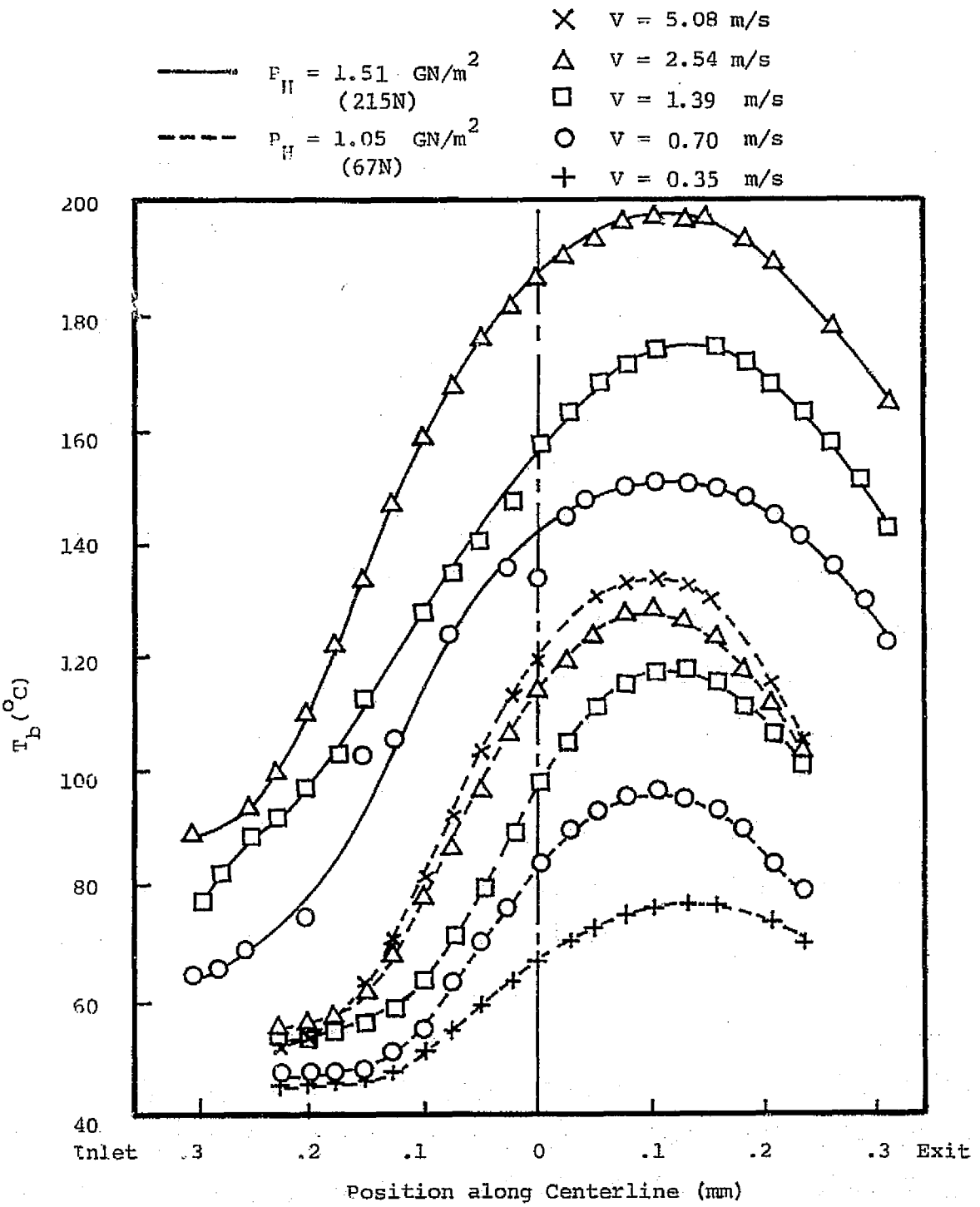

Figure 7. Ball Surface Temperature Along Centerline as a Function of Speed and Load - Naphthenic Base Oil N1, 40°C Bath Temperature, Smooth Ball (.011 μm c.l.a.).

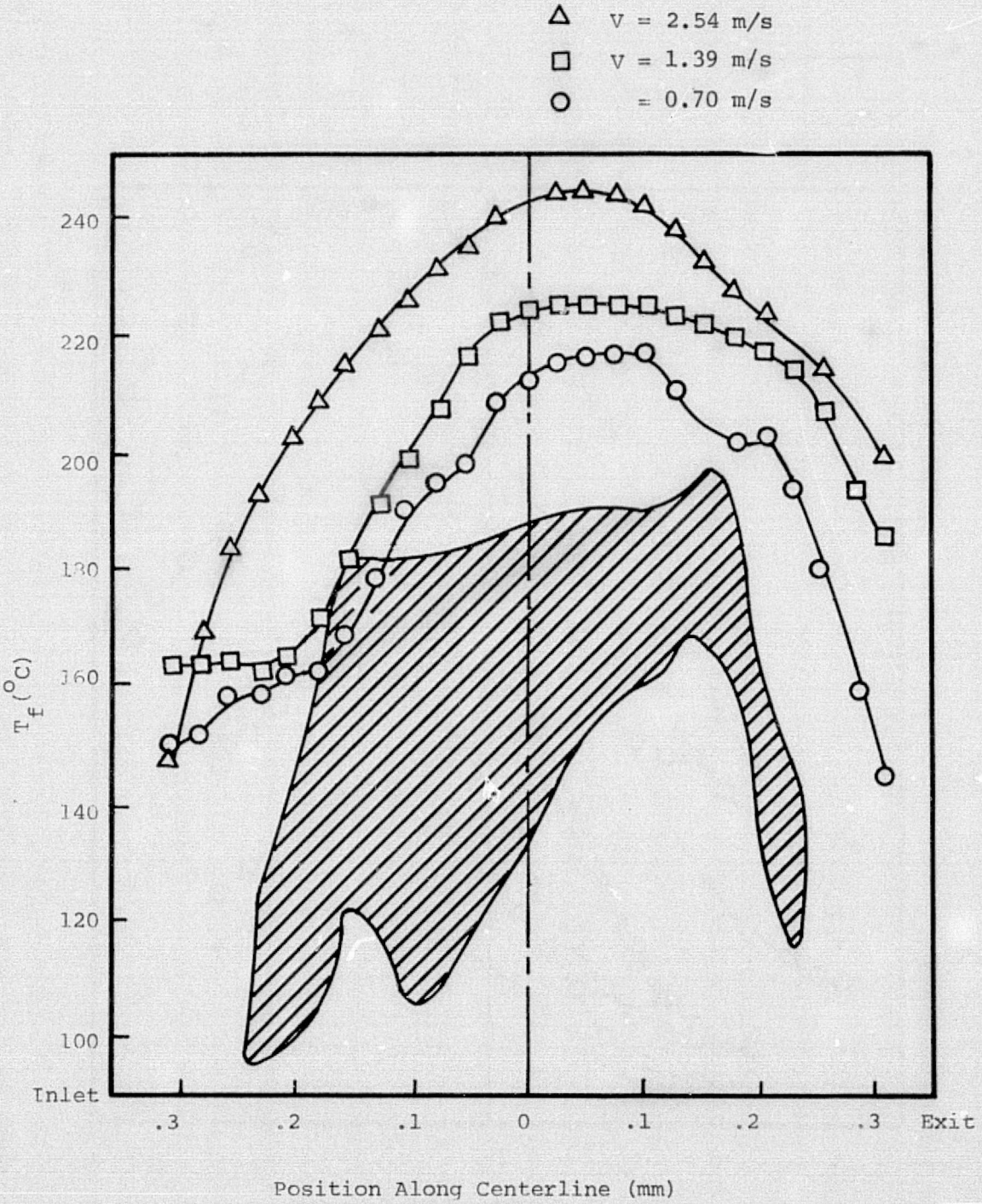

Figure 8. Average Fluid Temperature Along Centerline as a Function of Speed. P_H = 1.51 GN/m^2, Naphthenic Base Oil N1, 40°C Bath Temperature, Smooth Ball (.011 μm c.l.a.). Shaded area represents envelope of similar data taken at P_H = 1.05 GN/m^2 (ref. 10).

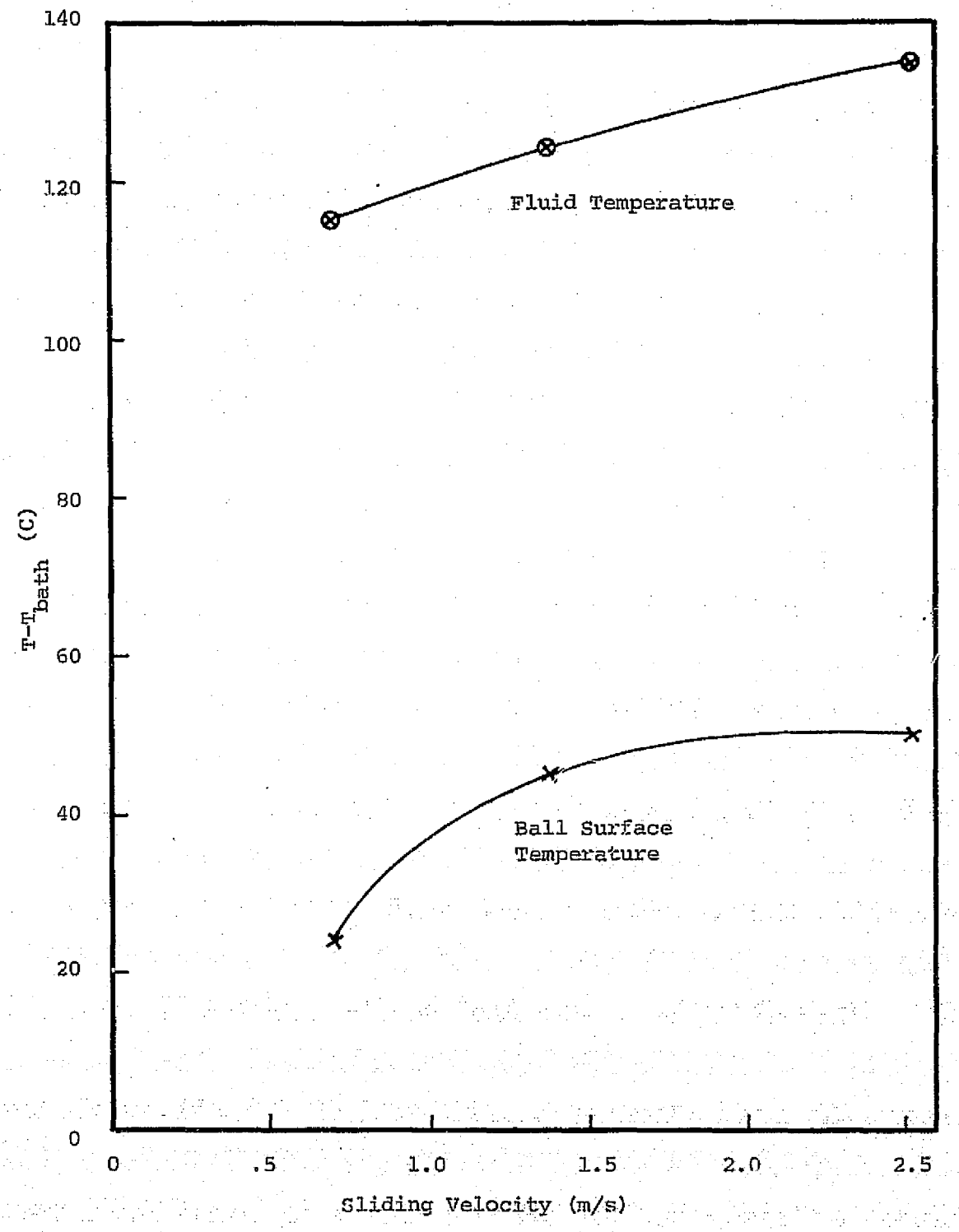

Figure 9. Temperature Increase above Bath Temperature at Contact Inlet - 1.51 GN/m^2 Hertz Pressure, Naphthenic Base Oil (N1), Smooth Ball (0.011 μm c.l.a.).

have been measured at the point of entry to the Hertzian contact zone. It is apparent that a significant amount of inlet heating has occurred. Inlet shear heating is important because it has a significant effect on the viscosity of the oil entering the contact and therefore, is instrumental in determining the film thickness. The inlet surface and fluid temperatures increase steadily with speed because the film thickness does not change appreciably with speed and consequently results in higher viscous dissipation at higher speeds.

B. Ball Surface Temperature Measurements Under Severe Conditions

In order to understand the failure of elastohydrodynamic films and the behavior of the contact temperatures, it is necessary to examine the EHD contact under conditions which result in relatively thin films, i.e. films of the same thickness as the composite roughness of the bounding surfaces. Under such circumstances, the fluid film may be locally discontinuous, resulting in ambiguous fluid temperature readings. Therefore, during this study, only the ball surface temperature was measured. In addition, for convenience, measurements were taken only at the center of the Hertzian contact. The temperature at the contact center is near the maximum (see Figure 7) and is, therefore, representative of the most severe conditions in the EHD contact.

Figure 10 shows a plot of the ball temperature rise at the contact center above the bath temperature, as a function of sliding velocity for peak Hertz pressures ranging from 0.52 to 2.03 GN/m^2. For a given Hertz pressure, the data plotted on log-log coordinates falls on one straight line for velocities up to a certain value and then on another line, of lower slope, for higher velocities. This decreasing dependence of temperature on velocity is supported, by the arguments of Archard [22] and Jaeger [23]. Applying Archard's analysis to a point contact results in the temperature difference between the fluid midplane temperature (assumed to be the maximum fluid temperature) and the ball surface temperature given by

$$T_f - T_b = \left(\frac{W}{4k_f \pi a^2}\right) (TC \cdot V \cdot h) \qquad (4)$$

For a given load, the fluid temperature rise is proportional to the product (TC·V·h). At Hertz pressures $\geq$ 1.5 GN/m^2, the film thickness and traction coefficients were essentially constant, resulting in a fluid midplane temperature rise which should be proportional to velocity. It is apparent that the ball surface temperature rise is less dependent on velocity (Figure 10) and that this dependence decreases with increasing velocity. Considering the fluid midplane as a heat source at temperature T_f, the ball surface temperature is a function of this temperature level and two characteristic times: the time constant for heat penetration to a depth of one contact radius below the ball surface t_1 is $(a^2 c_b \rho_b / 2k_b)$ and the characteristic fluid resident time t_2 is (a/V) [22]. For a given load and constant h, which is essentially true for P $\geq$ 1.5 GN/m^2, the ratio t_1/t_2 is directly proportional to velocity. For a given load, in fact, t_1 is essentially constant under these conditions, which implies that the diffusion rate into the ball is fixed, while the fluid resident time varies inversely with velocity. A point on the ball surface is then exposed for time t_2 to the fluid mid plane temperature level, which increases linearly with velocity, but the exposure time decreases with velocity. The net effect is a surface temperature with a decreasing slope as shown in Figure 10. The temperature rise shown in Figure 10 is the difference between the ball surface and lubricant bath temperatures.

Figure 10 also contains ball surface temperature data as a function of load. The same data, at selected velocities, is replotted in Figure 11 as a function of Hertz pressure. The temperature rise is the difference between the ball temperature at the contact center and the lubricant bath temperature as measured with a thermocouple. Figure 11 shows that except

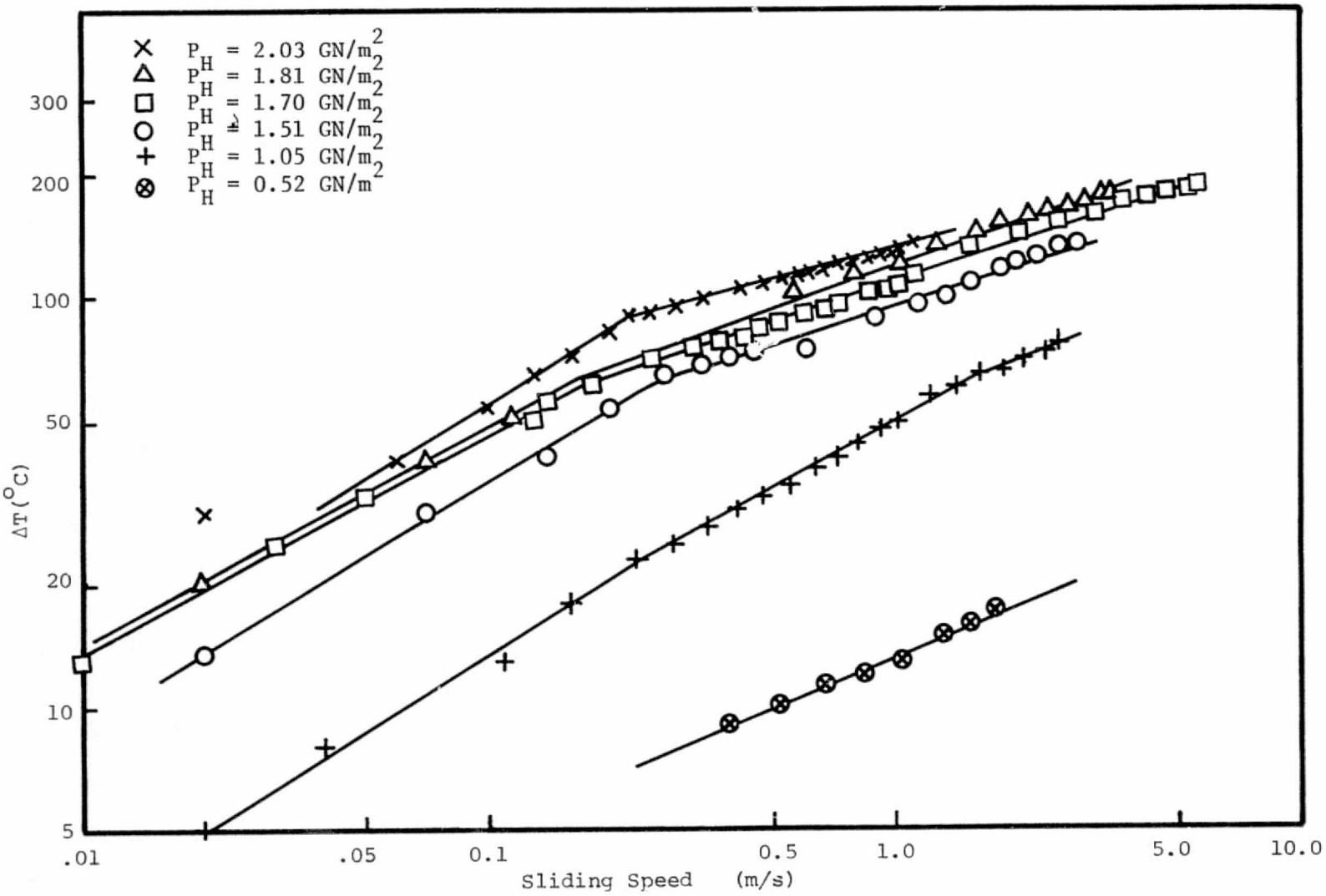

Figure 10. Ball Surface Temperature Rise at Contact Center, Smooth Ball (.011 μm c.l.a.), $1 < \Lambda < 2$ for P_H = 2.03 GN/m^2, otherwise $\Lambda > 2$.

for the combined conditions of relatively high velocity and high Hertz pressure, the data for a given speed follows a power law model with an exponent on Hertz pressure of approximately 2. Equation (4) can be rewritten in terms of Hertz pressure, resulting in

$$T_f - T_b \propto P_H V(TC \cdot h) \tag{5}$$

for a given fluid. The product (TC·h) depends on both P_H and V, but the dependence of the product on P_H is small. Therefore, holding V constant, (T_f-T_b) should be proportional to Hertz pressure to the first power. However, using the time ratio t_1/t_2, described above, the larger dependence on P_H of the ball surface temperature rise shown in Figure 11 can be quantitatively rationalized. Holding velocity constant, t_1/t_2 is proportional to the Hertz radius a which is directly proportional to P_H. The P_H axis in Figure 11 is also a t_1/t_2 axis for a given V. Since it has been argued that the heat source has a temperature rise proportional to P_H (equation 5), the temperature rise of the surface, will also depend on the relative values of t_1 and t_2. As P_H increases, t_1 increases as its square. This means that the effective heat diffusion into the ball is decreasing significantly and the surface temperature will remain relatively high. In addition, as P_H increases, t_1 increases proportionately. This results in a longer exposure time of the ball surface to the heat source. Therefore, although (T_f-T_b) rises linearly with Hertz pressure the ball surface temperature will rise significantly faster, because of both increasing fluid residence time and decreasing thermal diffusion.

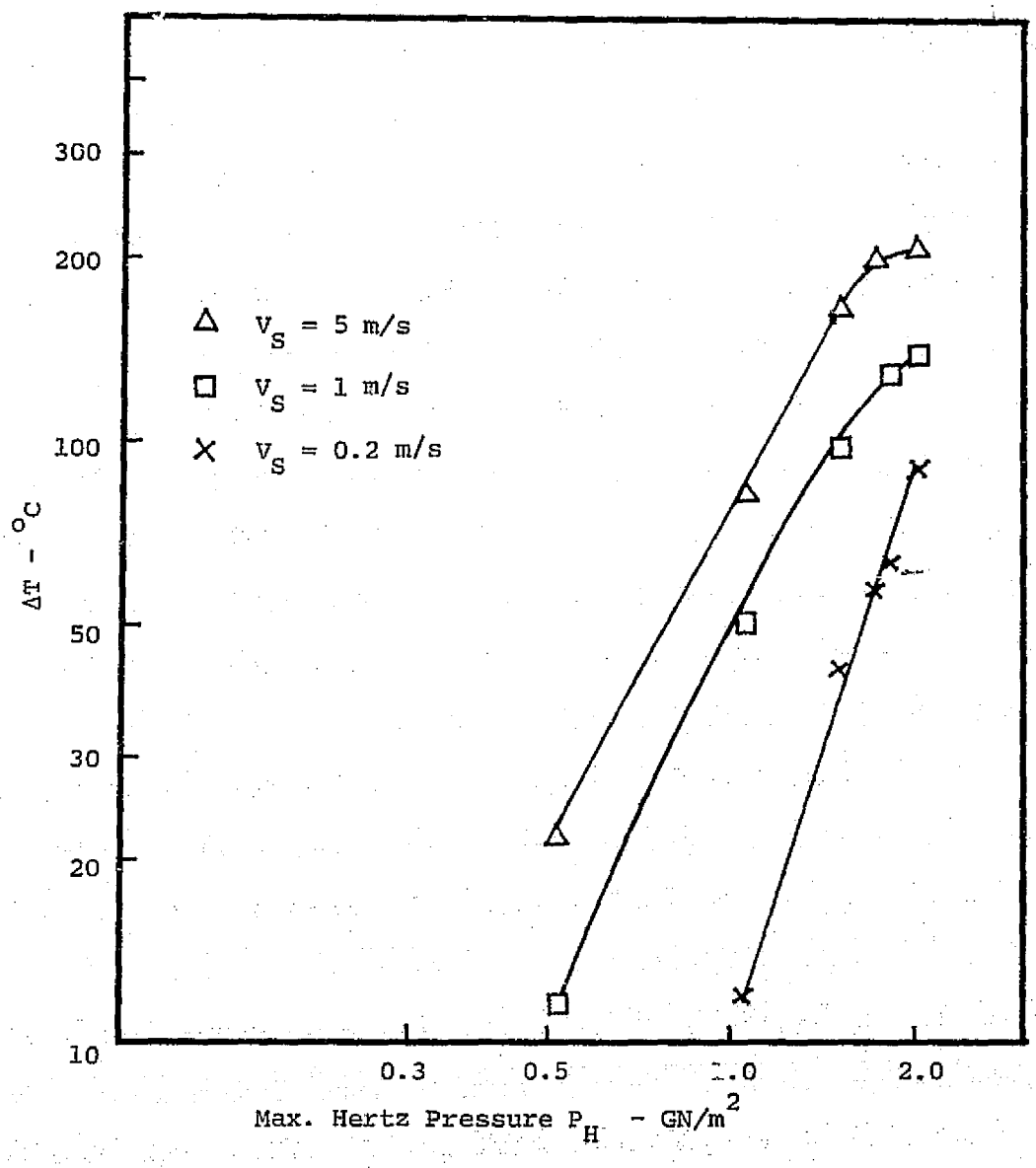

Figure 11. Surface Temperature Rise at Contact Center Versus Maximum Hertz Pressure, Smooth Ball (0.011 μm c.l.a.).

C. Comparison of Results with the Blok-Jaeger-Archard Flash Temperatures

A useful summary of the original flash temperature formulation of Blok [24] and the theoretical calculations of Jaeger [23] has been given by Archard [22] along with a graphical procedure for determining this temperature. In this section, a comparison of ball surface temperatures calculated using this method and those obtained experimentally has been made as shown in Figure 12. Agreement is good in most cases. The calculated values are contact average temperatures predicted by theoretical considerations. The measured values are either the temperature at the contact center when only such temperatures were recorded, or the mean of the highest and lowest temperatures in the Hertzian contact area when a temperature map was obtained. A regression analysis of measured temperatures on calculated temperatures resulted in a coefficient of determination of 0.85. Table II shows these temperatures as functions of Hertz pressure and sliding velocity.

It should be noted that the calculated temperatures were obtained by adding the bath temperature, as measured with a thermocouple, to the calculated temperature rise. The measured values, however, whether the centerline or contact average temperatures, are the values which result directly from the experimental data reduction. The measured values should be somewhat higher than the calculated values since both the lubricant and surface temperatures just outside the EHD contact are significantly higher than the bath oil temperature due to conduction and inlet heating.

The measured and calculated temperatures agree reasonably well both in magnitude and trend with increasing speed and load. Because it considers conduction as the only heat transfer mechanism, the flash temperature theory should best agree with experimental results at high pressures.

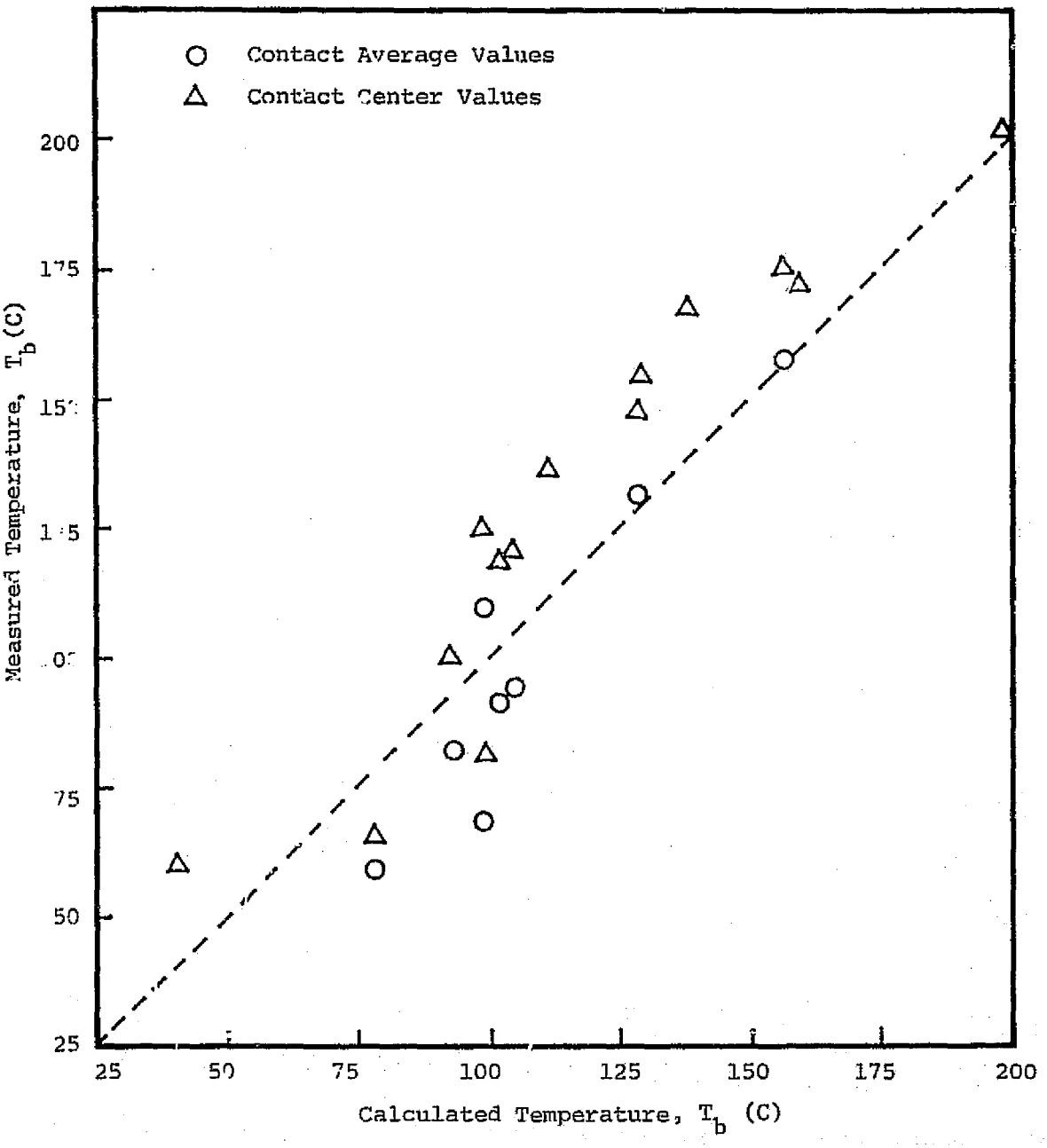

Figure 12. Comparison of Average Contact Temperatures Calculated Using the Blok Jaeger-Archard Theory and Measured Temperatures, Smooth Ball (0.011 μm c.l.a.).

Table II. Summary of Comparison of Measured Temperatures and Those Predicted by the Blok-Jaeger-Archard Theory for the Smooth Ball (0.011 μm c.l.a.).

P_H (GN/m^2)	V (m/s)	Traction Coefficient	Avg. Calculated Temperature (^oC)	Measured Center Temperature (^oC)	Avg. Measured Temperature (^oC)
2.03	1.0	0.07*	158.9	172	-
1.81	1.0	0.07*	137.5	167	-
1.70	0.05	0.07*	40	60	-
	1.0	0.07*	129	154	-
	2.54	0.07*	198	202	-
1.51	0.70	0.07	98	124	109.6
	1.0	0.07*	111	136	-
	1.39	0.07	128	147	131
	2.54	0.06	156	175	156.7
1.05	0.35	0.16	77.7	65	58.8
	0.70	0.13	98.4	81	68.4
	1.39	0.07	92.4	100	81.5
	2.54	0.06	101.2	118	90.8
	5.08	0.04	104.1	120	93.7

*Assumed value based on similar conditions

In these cases, the ratio of contact length to height is the greatest thereby making conduction more significant. This trend is supported by the data for P_H = 1.51 GN/m^2 and 1.05 GN/m^2, in which contact average measured temperatures have been determined. The average deviation between calculated and measured temperatures was 4.8% for the 1.51 GN/m^2 data and 17% for the 1.05 GN/m^2 data using a Celsius temperature scale.

Although the flash temperature concept offers a means of estimating the contact surface temperature it is subject to substantial limitations. The average value obtained can be significantly in error, but more important, the method yields only an average. The peak temperature, which may be more important in determining contact behavior, is often much higher than the average.

D. Surface Roughness Effects

To study the effect of surface roughness on ball surface temperature at the contact center, AISI 52100 chrome steel balls of different surface roughnesses were used in the EHD contact simulator. Up to this point, the center line average surface roughness of the steel balls has been .011 μm. The roughness characteristics of the balls used in all studies were independent of direction on the surface. This random orientation is a result of different lapping and polishing techniques.

Profiles of the sapphire surface and ball surfaces were measured using a Bendix Group XV System with a modified specimen holder to accommodate the curvature of the ball surfaces. The surface profiles are shown in Figure 13 for the sapphire surface and the three ball surfaces investigated. In addition to the .011 μm surface roughness ball, balls of .076 μm and .381 μm surface roughness are shown. The plots in Figure 13 do not all have the same vertical magnification, as noted. The curvature of the ball surface can also be seen at high magnification levels. In the following discussions, the .011, .076 and .381 μm surface roughness balls will be referred to as the smooth, medium rough and rough surface balls respectively.

Figures 10, 14 and 15 show ball surface temperatures at the center of the EHD contact as a function of speed and load for the smooth, medium rough and rough balls respectively. In addition, Figure 16 shows the temperature data replotted as temperature rise (difference between ball surface and bulk oil temperature) as a function of peak Hertz pressure and sliding speed. In the experiments with the rough ball, the temperature reported is the maximum in the contact, whether or not it occurs

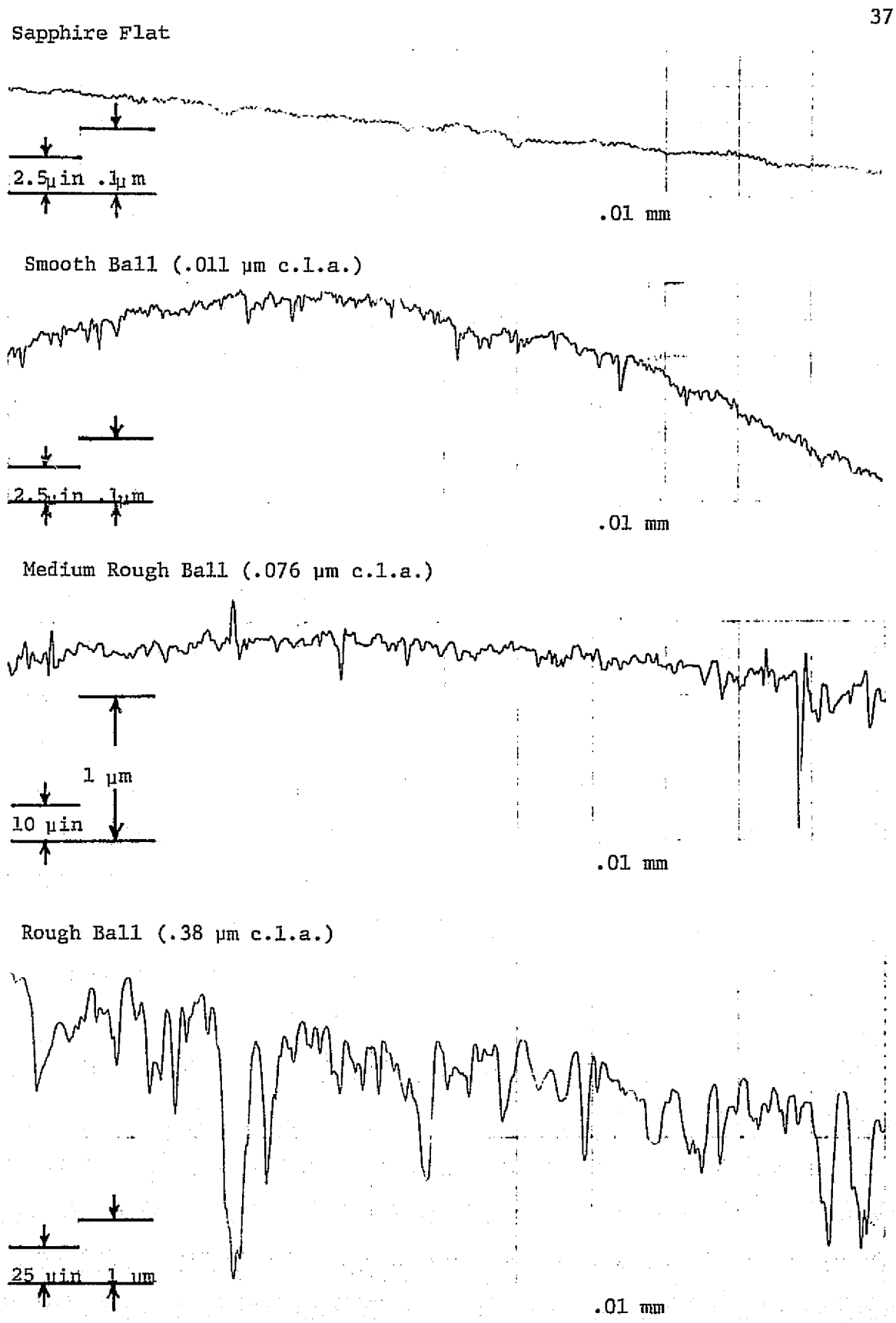

Figure 13. Surface Roughness Profiles.

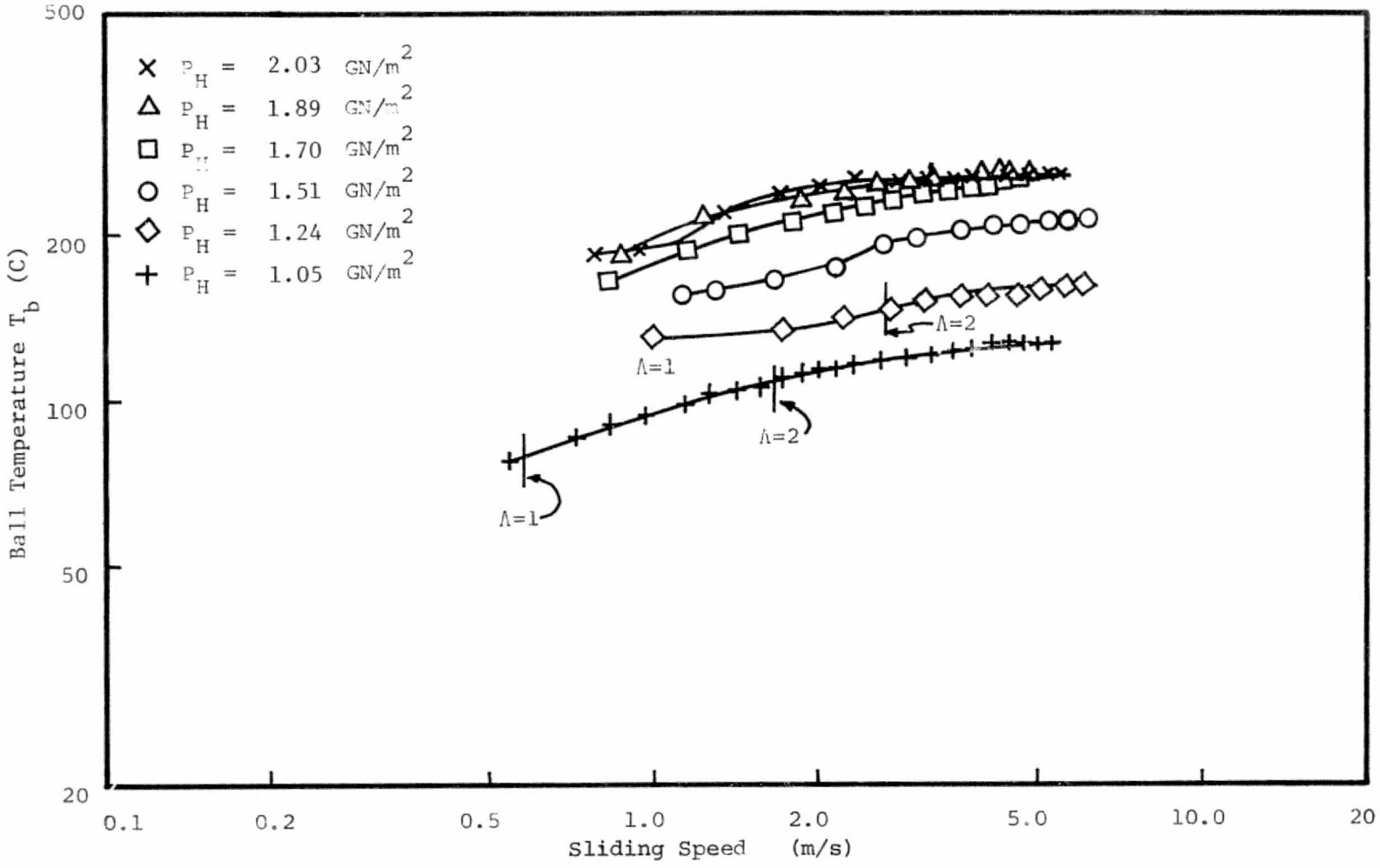

Figure 14. Ball Surface Temperature at Contact Center, Medium Rough Ball (.076 μm c.l.a.), ($\Lambda < 1$, except as noted).

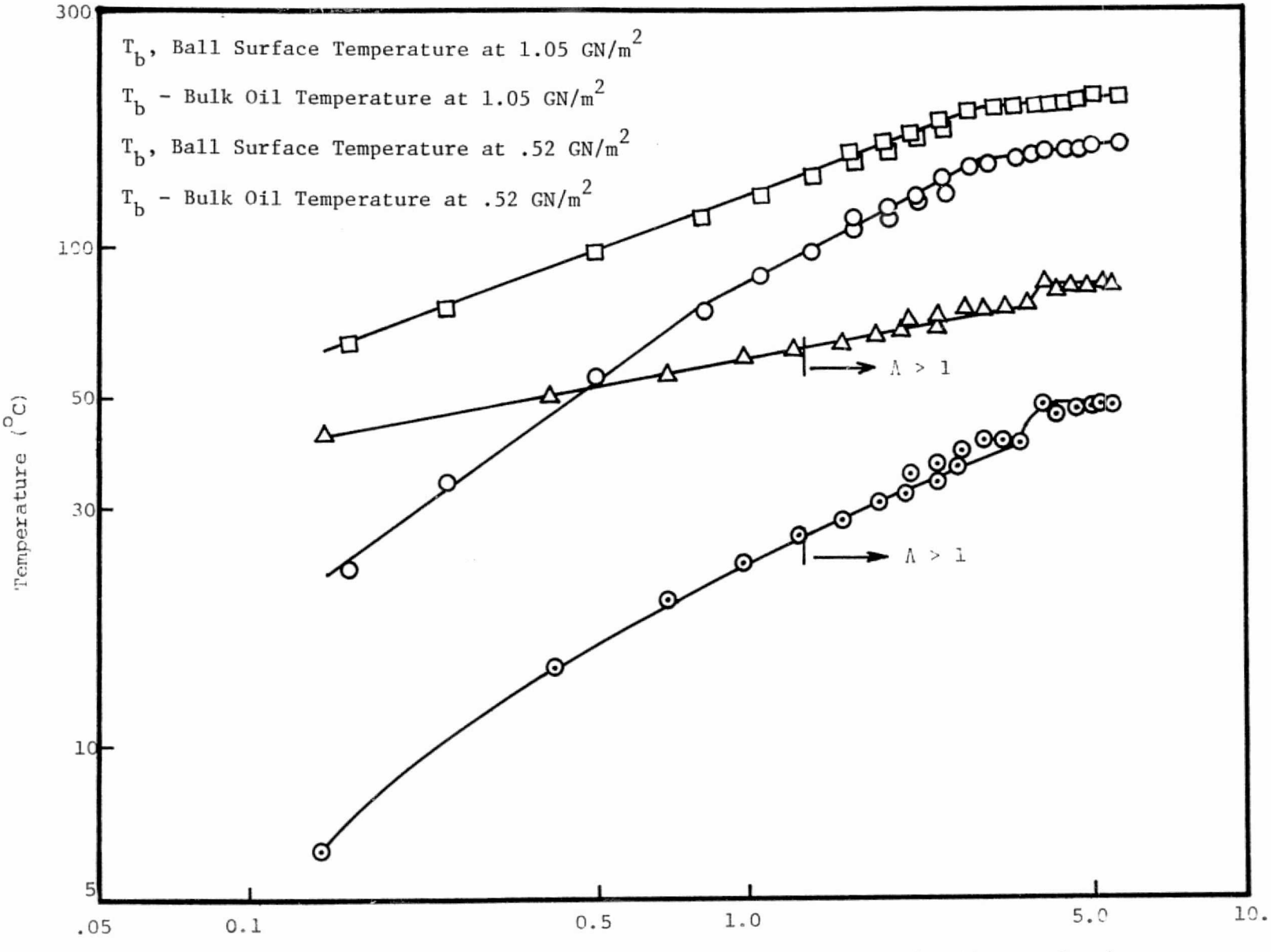

Figure 15. Maximum Ball Surface Temperature - Rough Ball (0.381 μm c.l.a.), (Λ < 1, except as noted).

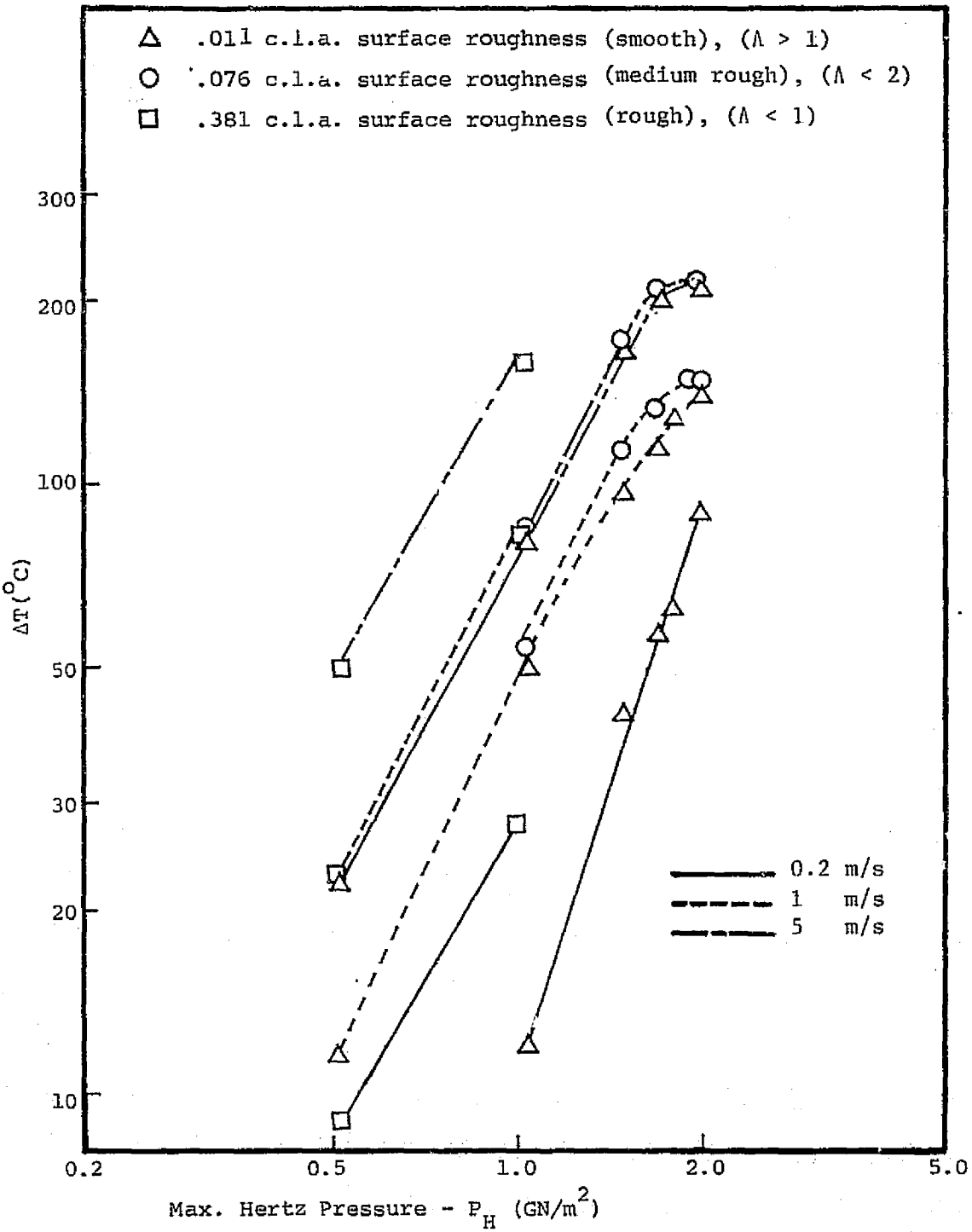

Figure 16. Ball Surface Temperature Rise versus Maximum Hertz Pressure.

at the contact center. It was necessary to make this procedural change because the contact center could not be located when the rough ball was used. This is due to the disappearance of the interference fringe pattern because of light scattering at the relatively large surface asperities. Therefore, the contact was scanned for the maximum surface temperature in each case.

The temperatures for the smooth and medium rough balls are only slightly different throughout the range of operating conditions. The surface temperatures for the rough ball appear to be significantly higher than those of the smoother balls. To put all temperatures on an equivalent basis the rough ball data in Figures 15 and 16 should be reduced by approximately $10^{\circ}C$. This is the difference between the maximum and center surface temperatures for the smooth ball (see Figure 3) .

The parameter Λ, which is the ratio of EHD film thickness h to the composite surface roughness σ, is a recognized parameter for predicting EHD contact performance [25]. For values greater than 2, no asperity interactions are expected. At Λ less than 1, severe asperity interaction is anticipated. The range $1 < \Lambda < 2$ is a transition region. Surface roughness measurements made on the sapphire and ball surfaces in this laboratory are c.l.a. values. The values of Λ obtained using c.l.a. rather than r.m.s. roughnesses are not sufficiently different that the transition values noted above are significantly altered [25]. Also, in computing the parameter Λ, the film thickness value used is that measured for the smooth ball. This is necessitated for two reasons. First of all the interference fringe pattern used to determine film thickness disappears as the roughness is increased. Secondly, the meaning of film thickness

is ambiguous at significant roughness levels, since the local thickness changes greatly from point to point. The appropriate Λ values are shown in Figures 10, 14-16.

In the case of the smooth ball, Λ is greater than 2 for Hertz pressures up to 1.810 GN/m^2, suggesting no asperity interaction. At P_H = 2.03 GN/m^2 Λ is in the range 1 to 2. However, a subsequent measurement of the surface profile (the method is discussed in the next section) did not reveal any surface alteration.

Experiments using the medium rough ball resulted in $\Lambda < 1$ for $P_H > 1.51\ GN/m^2$ and $1 < \Lambda < 2$ at lower pressures. Moderate to severe asperity interaction is therefore expected at all speeds and loads investigated. A relocation surface profile measurement was obtained and is shown in Figure 17. At a Hertz pressure of 1.70 GN/m^2 it can be seen that peaks have been removed in the wear track.

For the rough ball, Λ is less than one for all operating conditions. A profile measurement for P_H = 1.24 GN/m^2 and V = 5 m/s is shown in Figure 18. The removal of asperities is clearly visible on the trace. In addition, the alteration of the surface in the wear track could be visually detected.

The above observations reinforce the importance of the parameter Λ in describing the extent of asperity interaction. In addition, it is now apparent that significant asperity interaction will result in increased surface temperatures.

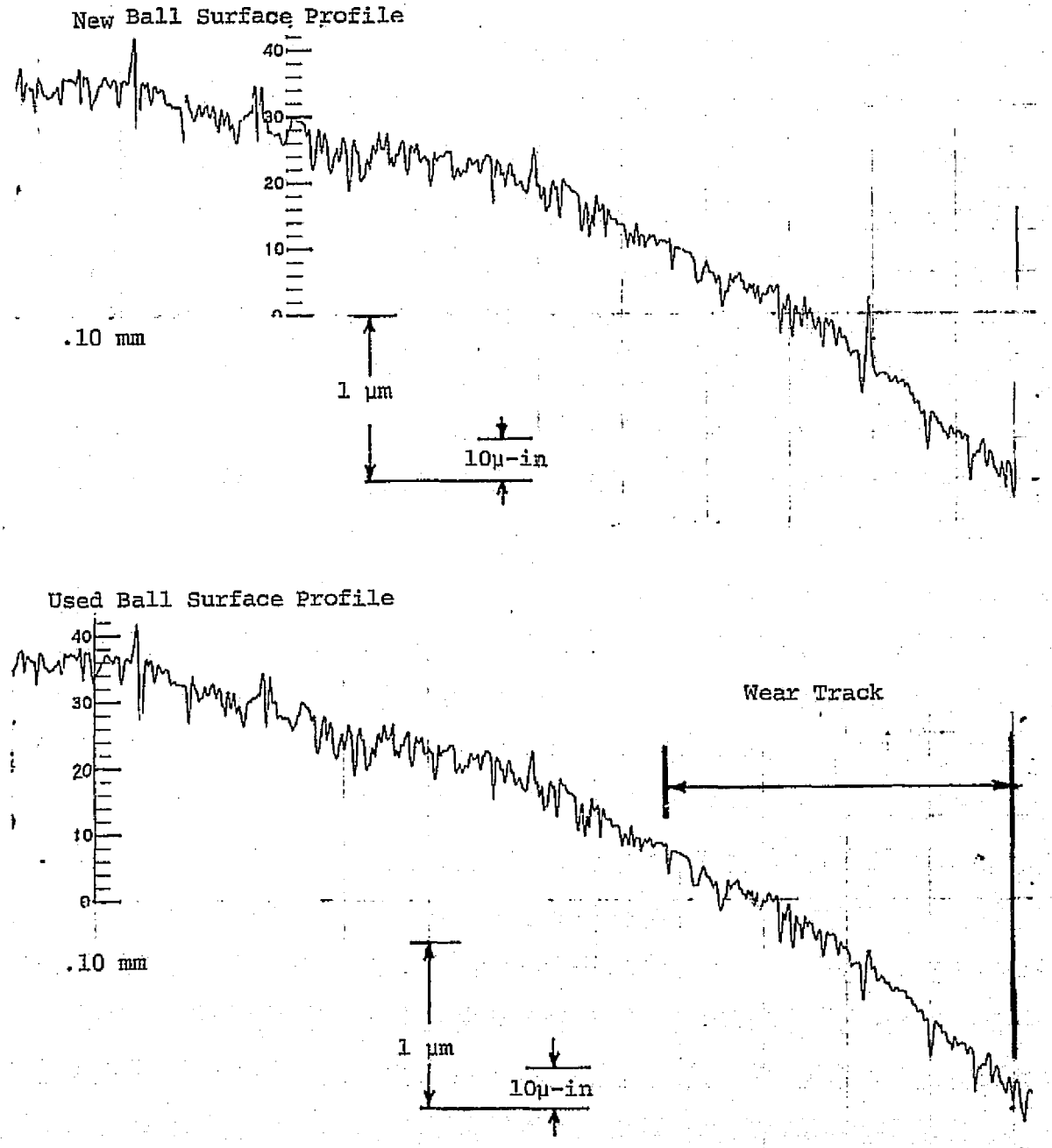

Figure 17. Relocation Profile for the Medium Rough Ball (.076 µm c.l.a.), (P_H = 1.70 GN/m^2, 0.83 $\leq$ V $\leq$ 5.0 m/s).

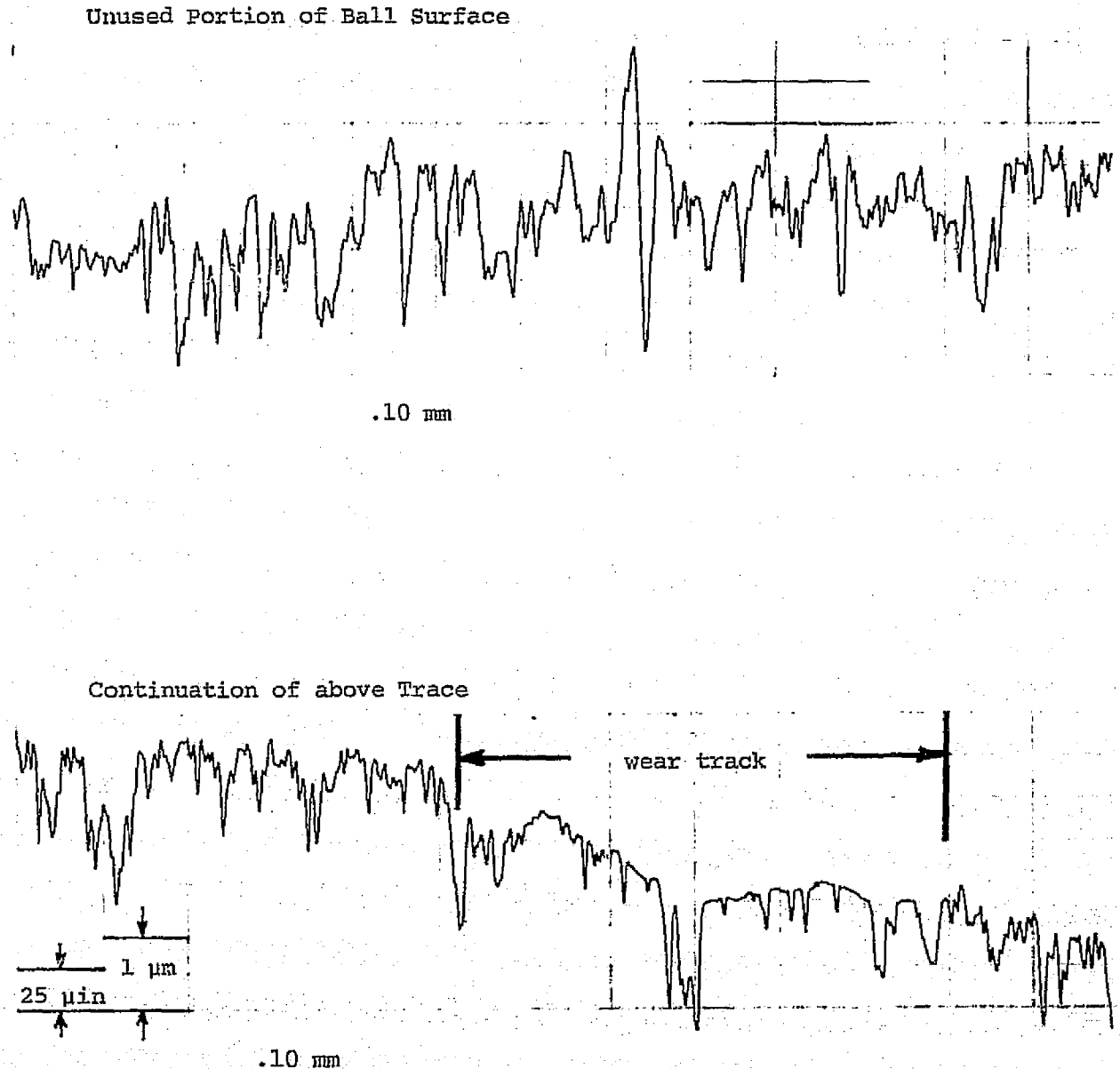

Figure 18. Surface Profile Showing Severe Wear, Rough Ball (.38 µm c.l.a.), 1.24 GN/m^2, 0.5 to 5.0 m/s Sliding Speed.

E. Relocation Profilimetry

Figure 19 shows two photographs of the specimen rotation attachment with a relocation stage fitted to a Bendix Group XV surface measuring system. Because of the curvature of the ball surface, it was necessary to modify the standard Bendix system to allow measurements over an adequate arc length at high vertical magnification. This has been accomplished by rotating the ball about its axis under a fixed stylus.

A relocation mechanism is incorporated in the rotation attachment. In order to detect any change in the surface profile, it is necessary to measure the profile at precisely the same point on the ball surface before and after being used in the EHD contact. Four of the possible six degrees of freedom are removed by using a pair of V-blocks to support the ball by two cylindrical collars cemented to the ball surface on opposite sides of the ball. The centerlines of the collars and ball are made as nearly coincident as possible. Since one of the collars is used to rotate the ball in the EHD contact simulator, the plane containing the wear track will be normal to this centerline. The other two degrees of freedom are removed by providing stops to limit motion along the axis of rotation and the amount of rotation about this axis.

As can be seen from Figure 17, the method has been successful in relocating the same area on the ball surface for re-examination. However, since it is not practical to obtain profiles of the entire wear track region before and after running in the EHD contact, an indication of no asperity interaction is inconclusive. Asperity interaction may have taken place at locations other than those measured.

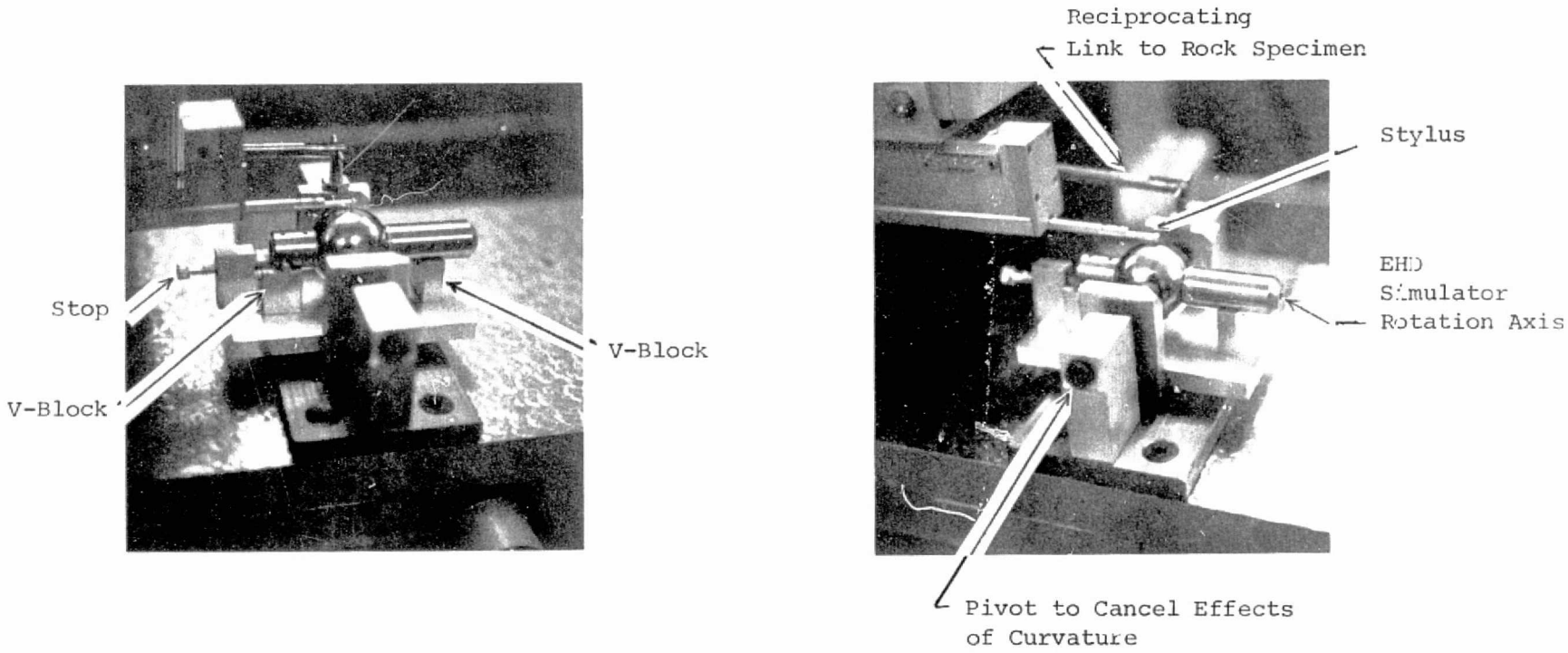

Figure 19. Surface Profilimetry Relocation Apparatus.

F. High Frequency Temperature Fluctuations

It has been demonstrated in the previous sections that asperity interaction can significantly alter the ball surface temperature level. The results given thus far, however, are time-averaged temperatures obtained with the infrared detector in the DC mode. In this mode of operation, the frequency response is 400 Hertz. From the surface profile measurements (Figures 17 and 18) it has been determined that only a single asperity can occupy the detector's field of view (.036 mm diameter) at any one time. However, at 1.0 m/s sliding velocity, the residence time is only 36 μs. The DC mode, therefore, cannot respond to a temperature rise caused by a single asperity interaction. The available AC mode of operation, however, can detect such temperature transients. The liquid nitrogen cooled detector has a response time of 8 μs. The differences in the AC and DC modes of operation are shown in Figure 20.

An important consequence of operating in the AC mode is that the reference signal is absent. Instead the instrument will produce a voltage difference proportional to the variation in target radiation emitted. Through an independent experiment, using an external chopper, it has been determined that the variation indicated in the AC mode is centered on the signal received in the DC mode. From this information a plot of time-averaged surface temperature along with the maximum and minimum values can be obtained.

Electrical noise problems were encountered when using the AC mode. A satisfactory solution was obtained, however, by using a variable electrical band pass filter. Although the noise and signal could not be entirely separated due to the closeness of their frequencies, a pass

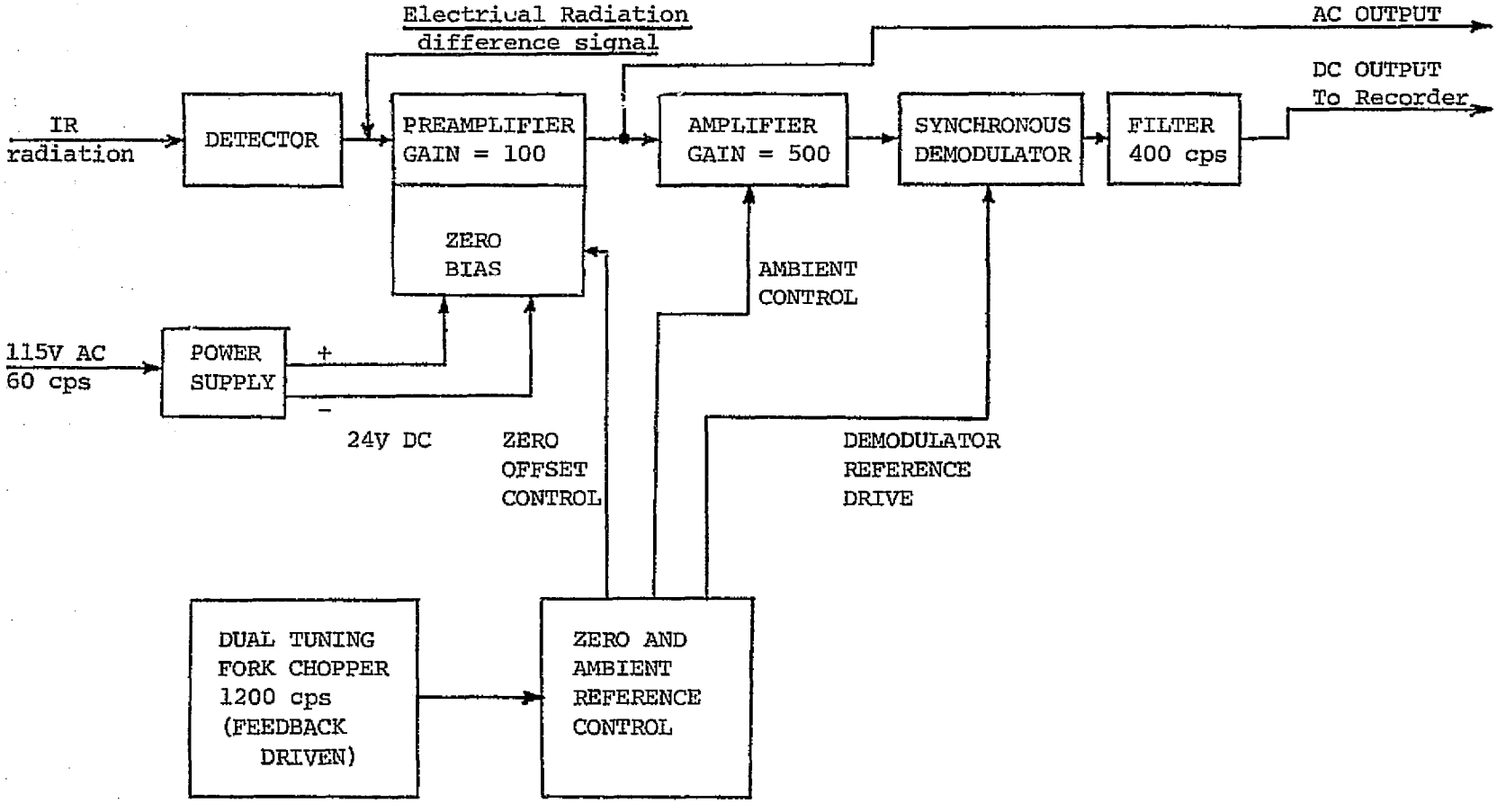

Figure 20. Block Diagram Showing Operation of Barnes RM-2A IR Microscope in Both DC and AC Modes.

band of 1.0 to 20 KHz proved effective, since the high peaks in the signal are within 20 KHz for most of the sliding speeds.

Figure 21 shows a plot of the ball surface temperature at the contact center as a function of Hertz pressure. The .076 μm c.l.a. surface roughness ball was used at a sliding speed of 1.0 m/s. The plot shown was constructed using the DC mode data at five different Hertz pressures. In addition, the AC mode was used at the four highest Hertz pressure levels. As is shown in Figure 21, the AC data shows no fluctuation about the DC level at $P_H = 1.05$ GN/m^2, but shows an increasing amount of fluctuation as the pressure is increased. The upper and lower curves represent the range of temperatures detected. It is believed that the peak values represent individual asperity interactions. Figure 21 also shows the significance of the parameter Λ in predicting the onset of asperity interaction. Figure 22 is a graph of the same data, along with data from higher sliding speeds. In all cases, the center value represents the DC (time averaged value). From this data it appears that the range of temperatures detected in the AC mode of operation increases significantly as more of the normal load is supported by individual asperities. This corresponds to a condition of decreasing Λ values.

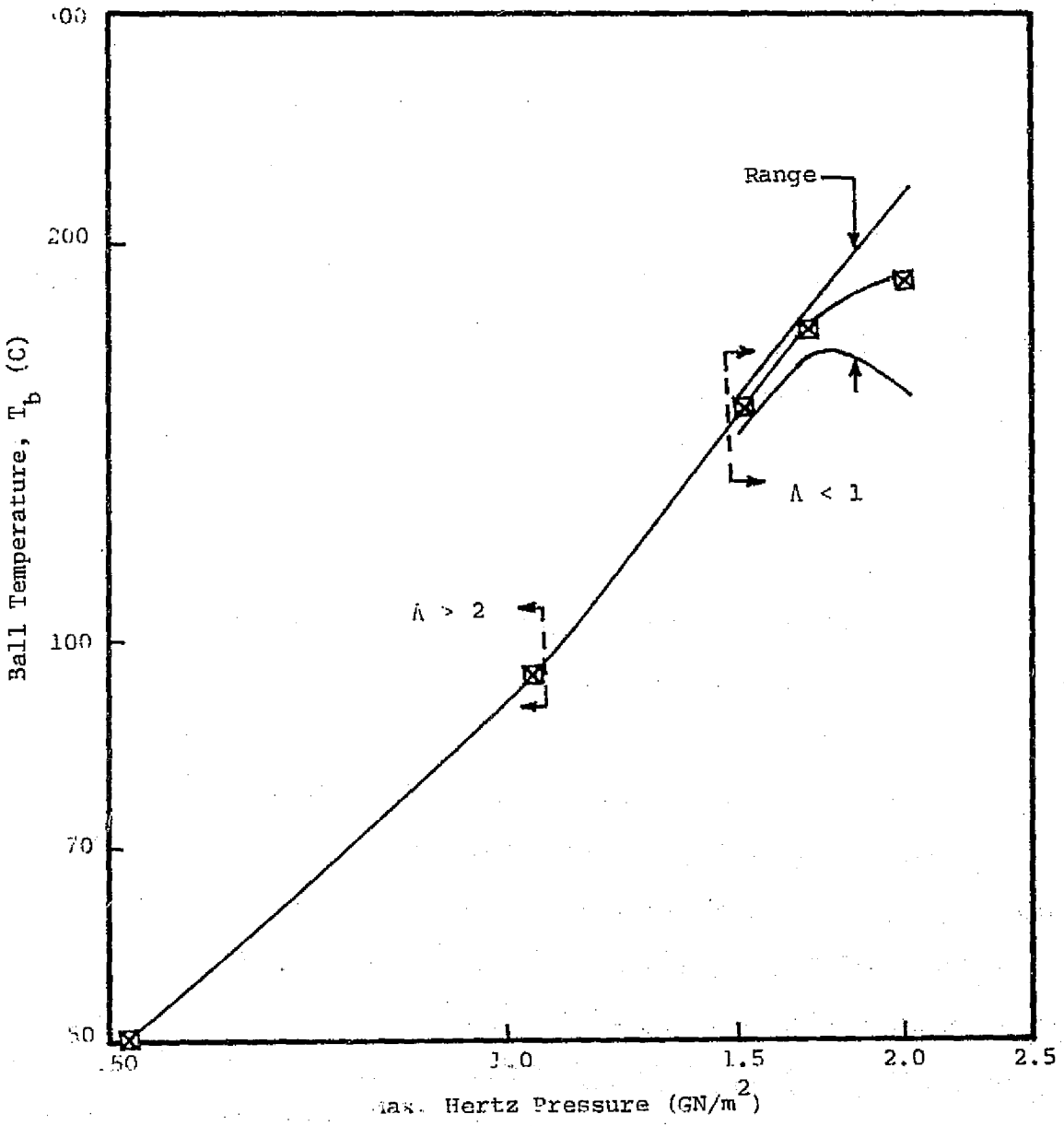

Figure 21. Average Value and Range of Ball Surface Temperature Fluctuation - Medium Rough Ball (.076 μm c.l.a.), 1.0 m/s Sliding Velocity.

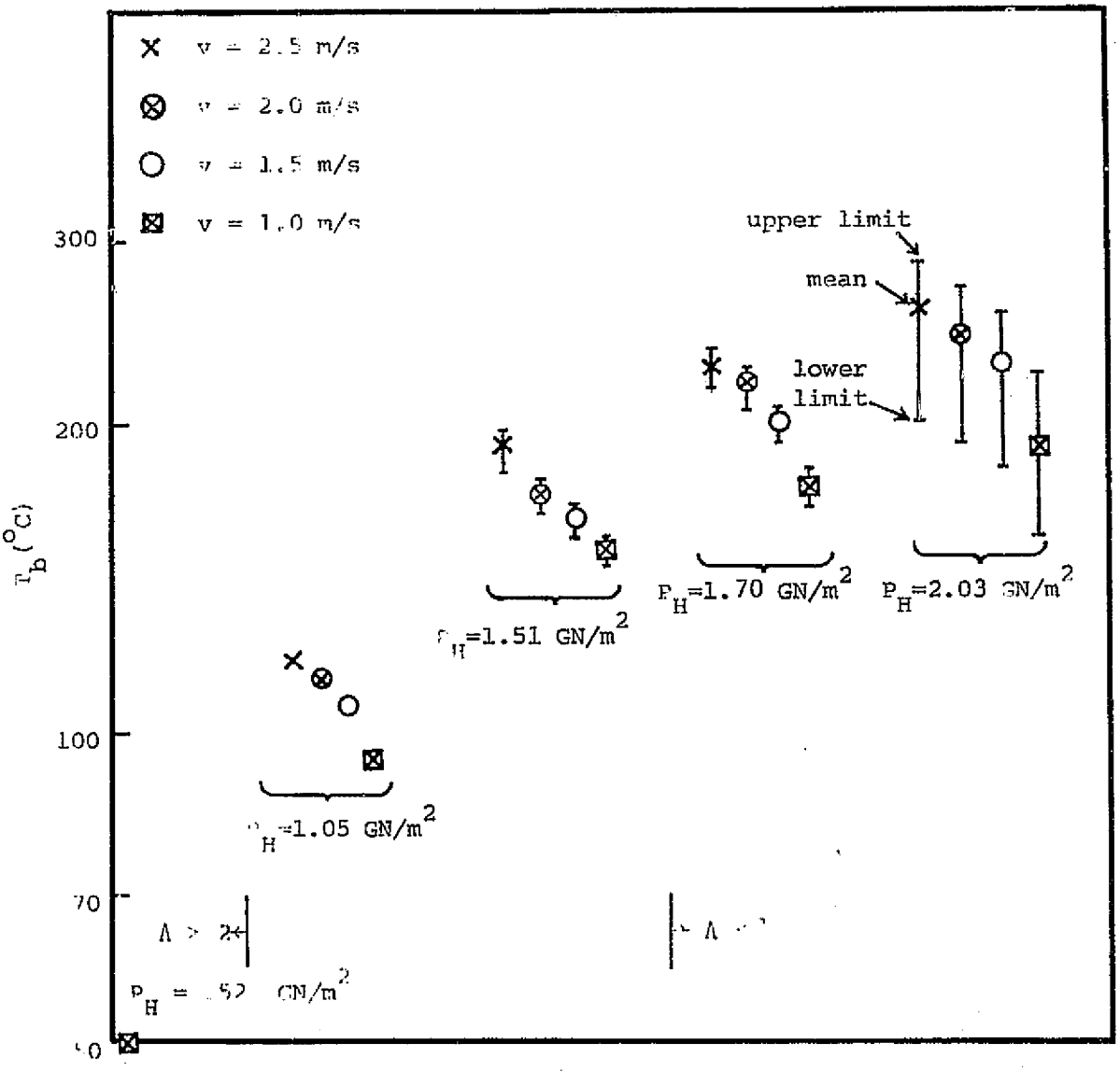

Figure 22. Average Value and Range of Ball Surface Temperature Fluctuations - Medium Rough Ball (.076 μm c.l.a.).

IV. REFERENCES

1. Crook, A. W., "The Lubrication of Rollers III: A Theoretical Discussion of Friction and Temperature in the Film," Phil. Trans. Roy. Soc. of London, A, 254, 1961.

2. Kannel, J. W. and Walowit, J. A., "Simplified Analyses for Tractions between Rolling-Sliding EHD Contacts," Trans. ASME Jolt, Series F, Vol. 93, No. 1, 1971.

3. Allen, C. W., Townsend, D., and Zaretsky, E., "Elastohydrodynamic Lubrication of a Spinning Ball in a Non-Conforming Groove," Trans. ASME, JOLT, Series F, Vol. 92, No. 1, 1970.

4. Turchina, V., Sanborn, D. M., and Winer, W. O., "Temperature Measurements in Sliding Elastohydrodynamic Point Contacts," Trans. ASME, JOLT, Series F, Vol. 96, No. 3, 1974.

5. Cheng, H. S., and Sternlicht, B., "A Numerical Solution for the Pressure, Temperature and Film Thickness between Two Infinitely Long, Lubricated, Rolling and Sliding Cylinders under Heavy Loads," Trans. ASME, Journal of Basic Engineering, Series D, Vol. 87, No. 3, 1965.

6. Cheng, H. S., "A Refined Solution to the Thermal-Elastohydrodynamic Lubrication of Rolling and Sliding Cylinders," ASLE Trans., Vol. 8, No. 4, 1965.

7. Trachman, E. G. and Cheng, H. S., "Thermal and Non-Newtonian Effects on Traction in Elastohydrodynamic Contacts", Elastohydrodynamic Lubrication: Second Symposium, I. Mech. E., Paper c37/72, April, 1972.

8. Archard, J. F. and Baglin, K. P., "Non-dimensional Presentation of Frictional Tractions in Elastohydrodynamic Lubrication - Part I Fully Flooded Conditions," Trans. ASME, JOLT, Vol. 97, No. 3, July 1975, pp. 412-423.

9. Jakobsen, J., "Lubricant Rheology at High Shear Stress," Doctoral Dissertation, Georgia Institute of Technology, Sept. 1973 and University Microfilms, Ann Arbor, Michigan, 1973.

10. Carlson, S., Jakobsen, J., Nagaraj, H. S., Molina-C, M. A., Sanborn, D. M., and Winer, W. O., "Investigations of Lubricant Rheology as Applied to Elastohydrodynamic Lubrication," NASA CR-134730, Sept. 1974.

11. Jakobsen, J. and Winer, W. O., "Traction of Elastohydrodynamic Contacts with Thermal Shearing Flow," Trans. ASME, JOLT, Vol. 97, 1975, pp. 424-429.

12. Jakobsen, J. and Winer, W. O., "High Shear Stress Behavior of Some Representative Lubricants," Trans. ASME, JOLT, Vol. 97, 1975, pp. 479-485.

13. Kunz, R. K., "Thermal and Traction Behavior in Sliding Elastohydrodynamic Contacts," M.S. Thesis, Georgia Institute of Technology, Atlanta, 1974.

14. Sanborn, D. M., and Winer, W. O., "Fluid Rheological Effects in Sliding Elastohydrodynamic Point Contacts with Transient Loading: 2-Traction," Trans. ASME, JOLT, Series F, Vol. 93, No. 3, 1971.

15. Sanborn, D. M. and Winer, W. O., "Fluid Rheological Effects in Sliding Elastohydrodynamic Point Contacts with Transient Loading: 1-Film Thickness," Trans. ASME, JOLT, Series F, No. 2, 1971.

16. Novak, J. D., "An Experimental Investigation of the Combined Effects of Pressure, Temperature, and Shear Stress upon Viscosity," Ph.D. Dissertation, University of Michigan, Ann Arbor, 1968.

17. Roelands, C. J. A., "Correlational Aspects of the Viscosity-Temperature-Pressure Relationships of Lubricating Oils," Doctor Ingenieur Dissertation, Technische Hogeschool te Delft, 1966.

18. Sibley, L. B., "EHD Techniques and Application to the Design of Roller Bearings," Report No. A171Q010, SKF Industries, Inc., Research Laboratory, 1971.

19. Johnson, K. L. and Roberts, A. D., "Rheology of Oil Films at High Contact Pressure," Nature, Vol. 240, No. 5383, 1972.

20. ASME, Pressure-Viscosity Report, Vols. I and II, a report prepared by the ASME Research Committee on Lubrication, N. Y., 1953.

21. Ausherman, V. K., Nagaraj, H. S., Sanborn, D. M., and Winer, W. O., "Infrared Temperature Mapping in Elastohydrodynamic Lubrication," ASME Paper to be presented at Joint ASME-ASLE Lubrication Conference, Miami Beach, Florida, October 1975.

22. Archard, J. F., "The Temperature of Rubbing Surfaces," Wear, Vol. 2, No. 6, October 1959, pp. 438-455.

23. Jaeger, J. C., "Moving Sources of Heat and the Temperature at Sliding Contacts," Proc. Roy. Soc. N.S.W., Vol. 56, 1942, p. 203.

24. Blok, H., "Surface Temperatures under Extreme-Pressure Lubricating Conditions," Second World Petroleum Conference, Paris, June 1937, Vol. 3, Section 4.

25. Bamberger, E. N., et al., "Life Adjustment Factors for Ball and Roller Bearings - An Engineering Design Guide," ASME, New York, 1971.